Subsurface Storage of Freshwater in South Florida: A Digital Model Analysis of Recoverability

United States Geological Survey Water-Supply Paper 2261

Prepared in cooperation with the U.S. Army Corps of Engineers

Subsurface Storage of Freshwater in South Florida: A Digital Model Analysis of Recoverability

By MICHAEL L. MERRITT

Prepared in cooperation with the
U.S. Army Corps of Engineers

U.S. GEOLOGICAL SURVEY WATER-SUPPLY PAPER 2261

DEPARTMENT OF THE INTERIOR
DONALD PAUL HODEL, Secretary

U.S. GEOLOGICAL SURVEY
Dallas L. Peck, Director

UNITED STATES GOVERNMENT PRINTING OFFICE: 1985

For sale by the Distribution Branch, U.S. Geological Survey,
604 South Pickett Street, Alexandria, VA 22304

Library of Congress Cataloging in Publication Data

Merritt, Michael L.
Subsurface storage of freshwater in south Florida.

(Water-supply paper / United States Geological Survey ; 2261).
"Prepared in cooperation with the U.S. Army Corps of Engineers."
Bibliography: p.
Supt. of Docs. no.: I 19.13:2261.
1. Water, Underground—Florida—Artificial recharge—Mathematical models. 2. Water-storage—Florida—Mathematical models. I. United States. Army. Corps of Engineers. II. Title. III. Series: Geological Survey water-supply paper ; 2261.
TC801.U2 no. 2261 553.7'0973 s [627.56] 84-600116
[TD404]

CONTENTS

FIGURES

TABLE

Subsurface Storage of Freshwater in South Florida: A Digital Model Analysis of Recoverability

By Michael L. Merritt

Abstract

As part of a study of the feasibility of recovering freshwater injected and stored underground in south Florida, a digital solute-transport model was used to investigate the relation of recovery efficiency to the variety of hydrogeologic conditions that could prevail in brackish artesian aquifers and to a variety of management alternatives. The analyses employed a modeling approach in which the control for sensitivity testing was a hypothetical aquifer considered representative of permeable zones in south Florida that might be used for storage of freshwater. Parameter variations in the tests represented possible variations in aquifer conditions in the area. The applicability of the analyses to south Florida limestone aquifers required the assumption that flow nonuniformities in those aquifers are small on the scale of volumes of water likely to be injected, and that their effect could be represented as hydrodynamic dispersion.

Generally, it was shown that a loss of recovery efficiency is caused by (1) processes causing mixing of injected freshwater with native saline water (hydrodynamic dispersion), (2) processes causing the more or less irreversible displacement of the injected freshwater with respect to the well (buoyancy stratification, background hydraulic gradients, and interlayer dispersion), or (3) processes causing injection and withdrawal flow patterns to be dissimilar (directionally biased well-bore plugging, and dissimilar injection and withdrawal schedules in multiple-well systems). Other results indicated that recovery efficiency improves considerably with successive cycles, providing that each recovery phase ends when the chloride concentration of withdrawn water exceeds established criteria for potability (usually 250 milligrams per liter), and that freshwater injected into highly permeable or highly saline aquifers (such as the "boulder zone") would buoy rapidly.

Many hydrologic conditions were posed for model analysis. To have obtained comparable results with operational testing would have been more costly by orders of magnitude. The tradeoff is that the validity of results obtained from computer modeling is somewhat less certain. In particular, results must be qualified with observations that (1) the complex set of processes lumped as hydrodynamic dispersion is represented with a somewhat simplified mathematical approximation, and (2) other flow processes in limestone injection zones are as yet incompletely understood. Despite such reservations, the study is considered a practical example of the use of transport models in ground-water investigations.

INTRODUCTION

The continuing rapid urbanization of south Florida places an increasing burden on the system of public water supply, and there is concern whether future needs of the public will be satisfied. An important component of the water-management system is its capacity for storage in reservoirs such as Lake Okeechobee and the water-conservation areas, from which a network of canals delivers needed water to coastal urban areas during dry periods and discharges excess storage to the ocean during wet periods (Leach and others, 1972; Klein and others, 1974). These surface storage areas may become inadequate, as their enlargement is limited by the flat topography of the area, the growing scarcity of available land, and the desire to preserve wilderness and wetlands. The topography and climate are also responsible for substantial losses of water from surface reservoirs by evapotranspiration and seepage.

One method of increasing storage is the "subsurface storage alternative," a proposal that confined aquifers having suitable hydraulic properties but containing water unusable for public supply because of high mineral content be used as storage receptacles. In this report, ground water is referred to as saline and is considered nonpotable (U.S. Environmental Protection Agency, 1977) if its chloride concentration exceeds 250 mg/L, as it does in most artesian zones in south Florida.

The source of freshwater for injection would be surplus surface water available during the annual wet season or ground water from surficial aquifers (such as the Biscayne aquifer) which are easily replenished by rainfall. The term "cyclic injection" implies that injection and recovery might be done annually, with injection of surplus freshwater during the wet season followed by a short storage period and subsequent withdrawal of the injected freshwater as needed during the dry season.

Hydrogeologic and chemical characteristics of the aquifers may greatly affect the recoverability of potable water, as may the design of systems of wells and their operational regimes. Since an evaluation of the feasibility of the cyclic injection concept requires an understanding of these effects, their relation to recoverability has been

studied with computerized mathematical models as part of the U.S. Geological Survey study of cyclic injection. This study was undertaken in cooperation with the U.S. Army Corps of Engineers, which is responsible for assessing the feasibility of the subsurface storage alternative for south Florida. Other aspects of the study concerned the availability of surplus freshwater (Sonntag, 1984), potable water deficiencies motivating the development of water-supply alternatives, location of suitable injection zones, geologic testing and site evaluation, system design and construction, and operational problems such as well-bore plugging. These topics are discussed in a report prepared by Merritt and others (1983).

Purpose and Scope

Computer modeling was chosen as the means of studying aspects of cyclic injection because of its cost effectiveness relative to the performance of actual operational tests. This technique did, however, require model application of an innovative nature, with little specific guidance from previous studies. This report, thus, has a trifold purpose: to (1) document the approach and techniques used in the study so that results can be replicated by other investigators; (2) report the specific results of the study to the U.S. Army Corps of Engineers, which is responsible for determining the feasibility of the concept within the study area (fig. 1)—that part of south Florida underlain by saline artesian zones; and (3) report advances in the modeling of injection and withdrawal to those segments of the professional community concerned with the physics of injection processes, interaction of fluids of contrasting density, freshwater injection and recovery, and the digital modeling of variable-density solute transport.

The first objective requires documentation of parameter value assignments and the method of designing the various model analyses. The second objective requires a concise presentation of the results and an explanation of their significance for cyclic injection in the study area. The third objective requires a brief description of the model used, which embodies a state-of-the-art method of solute-transport simulation that has not been widely applied. It also requires that hydrologic concepts and modeling results be presented with adequate detail for the professional audience. Also included are discussions of model application techniques and means of overcoming various problems inherent in the model.

The report includes descriptions of analyses of various aspects of the relation of recoverability to hydrogeologic parameters and to system design and management parameters. The analyses are grouped into 12 somewhat interrelated categories to organize the report. Because of the report's comprehensive scope, every effort has been made to make the presentation concise and readable without omitting details of interest and value.

The report relates to the overall study of cyclic injection as a supporting document providing details of work briefly summarized in a more general report (Merritt and others, 1983) and is, therefore, intended for a somewhat specialized audience. Results are also summarized in the Proceedings of the American Society of Civil Engineers National Specialty Conference held in Orlando, Fla., July 1982 (Merritt, 1982).

Results of the study may have transfer value to other geographical areas because the assumption of uniform flow may apply to aquifers composed of material other than the limestone of aquifers of south Florida, for which this assumption is considered only approximately true. Results of the analyses do not apply to any site-specific management or feasibility problem. This is consistent with the theoretical goals of the analysis. However, site-specific or problem-specific analyses can be made with the same modeling techniques, provided adequate data are available.

Previous Studies

Kimbler and others (1975) developed theoretical equations relating the various processes controlling and limiting the recoverability of freshwater in a vertically uniform aquifer. Construction of a physical model permitted partial verification of the theoretical results. Their methods were implemented by Khanal (1980) in a theoretical investigation of injection feasibility in the Upper East Coast Planning Area for the South Florida Water Management District.

The subsurface waste disposal model (INTERCOMP Resource Development and Engineering, Inc., 1976) was used to simulate cyclic injection by D. B. Grove and L. F. Konikow of the U.S. Geological Survey, and their work was the subject of a paper presented at a meeting of the American Geophysical Union during December 1976 in San Francisco, Calif. (Grove and Konikow, 1976).

Acknowledgments

The study benefited from the help of Fred Meyer of the Miami subdistrict of the U.S. Geological Survey, who conducted the freshwater injection and recovery tests at Hialeah in Dade County. Meyer provided technical guidance at an early stage of the project that enabled the author to proceed with the theoretical analysis of freshwater injection, and his suggestions throughout were very helpful. Howard Klein, also of the Miami subdistrict, provided advice concerning the project reports. Recognition is due Rhonda Howard of the same office for her swift and efficient processing of this manuscript.

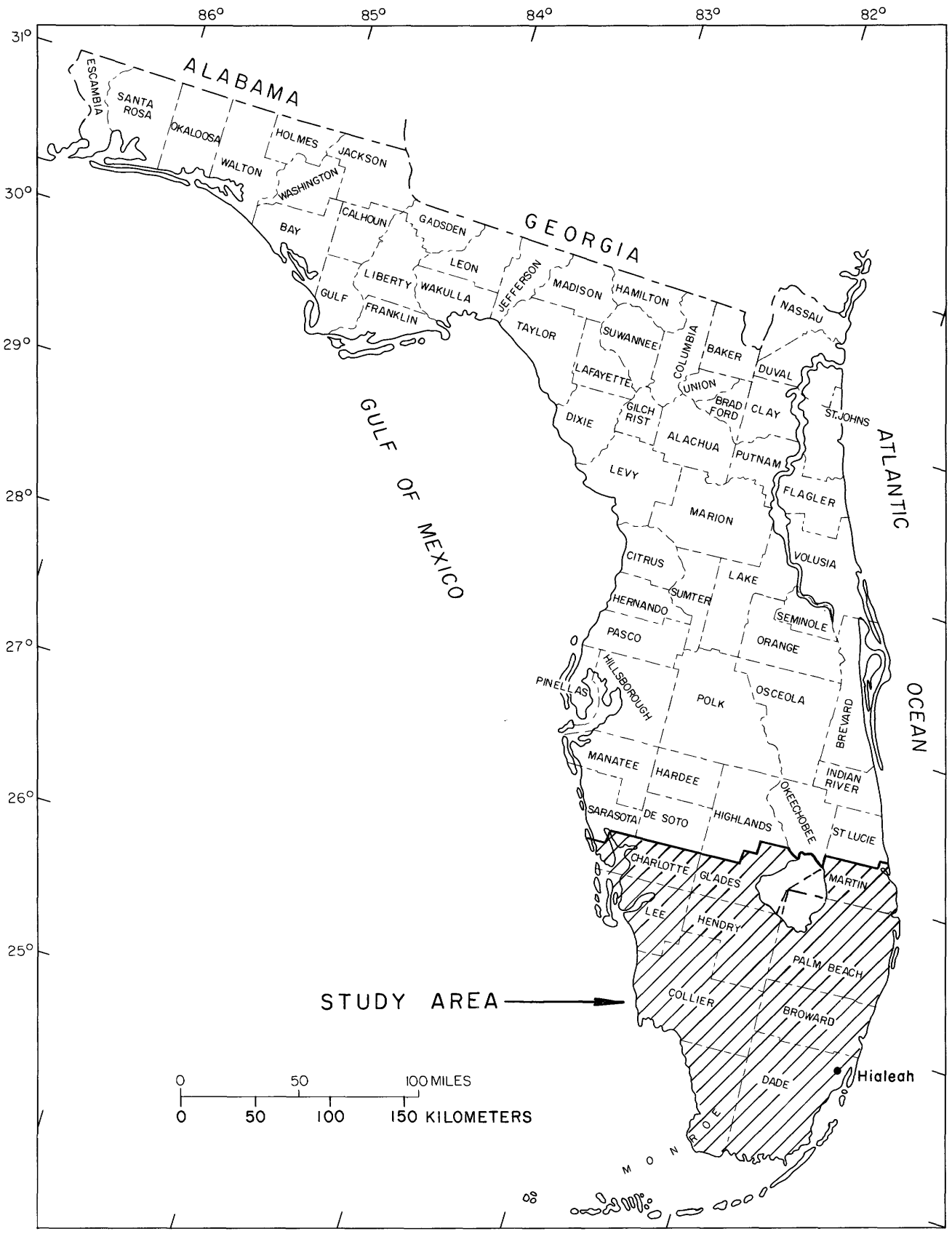

Figure 1. Location of study area.

Various forms of consultative assistance were provided by present and former members of the national research program of the U.S. Geological Survey: Steven P. Larson (former) and Leonard F. Konikow of Reston, Va., and David B. Grove and Kenneth L. Kipp of Denver, Colo.

The U.S. Geological Survey appreciates the support of Toney Lanier of the U.S. Army Corps of Engineers in helping the author achieve the objectives of the project.

Approach

Several physical processes that restrict the recoverability of injected freshwater have been identified: dispersion, buoyancy stratification, changes in directional permeability during injection or withdrawal, and downgradient displacement by the local background flow system. The recoverable amount of injected freshwater may be measured in terms of "recovery efficiency." Recovery efficiency is defined for each cycle as the volume of water recovered before its increasing chloride concentration exceeds the potability limit of 250 mg/L, expressed as a percentage of the volume injected.

Recovery efficiency, and other variables describing the processes of freshwater injection and withdrawal, can be calculated with available digital methods, given a set of parameter values describing hydrogeologic characteristics. If the parameters and model assumptions match hydrogeologic conditions in an aquifer, this process is simulation modeling and the computed hydraulic and chemical variables, including amount recovered, should closely match data acquired during actual injection and withdrawal. Such realistic simulation of nature is the most difficult task addressable by modeling, as it requires a complete set of accurate data describing natural processes. Such data are rarely available, particularly data describing the complex processes of solute transport in heterogeneously layered artesian aquifers of south Florida, which are carbonates characterized by many types and degrees of solution development, and in which flow may be anisotropic.

Objectives for modeling other than exact simulation or prediction can be defined that provide useful information and require considerably less data. Freshwater injection and withdrawal in a hypothetical geologic sequence resembling some known artesian injection zone in south Florida may be simulated using parameters generally similar to those of the aquifer. This approach may be termed "conceptual modeling" (Wheatcraft and Peterson (1979) use the term "interpretive model"). Sensitivity analyses determine how much the system response, in terms of recovery efficiency, varies when hydrogeologic or management parameters are varied. These analyses show the degree to which recovery efficiency will vary when differences in hydrogeologic conditions or operational techniques are represented by the parameter variations.

In this study, hydrogeologic and operational parameters describing the first injection test at Hialeah (fig. 1) in Dade County (F. W. Meyer, oral commun., 1980) were used as the control for sensitivity testing. In some cases, reasonable estimates based on limited data could be made (permeability stratification), and these were incorporated into the prototype. However, no data describing other hydrogeologic conditions (flow anisotropy or the degree of dispersive mixing of injected and native waters) were available. Few data describing typical degrees of hydrodynamic dispersion and its variability among the dissimilar artesian limestones of south Florida were available from previous studies. Because it was possible that sensitivity test results could depend to a great degree on the hydrodynamic dispersion parameters, several control simulations were designed. Each simulation incorporated a dispersion model (a hypothetical degree of dispersion represented by the parameter choices) significantly different from the others, and each was used for a complete series of tests of variations of other parameters. One dispersion model, that of little or no lateral dispersion, could not be incorporated into a control simulation because of the numerical limitations of the model.

All control simulations assumed that isotropic conditions prevailed. Special simulations were designed to determine how recovery efficiency would vary from that of an isotropic control simulation if anisotropic conditions actually prevailed at a cyclic injection site owing to natural features of the rock (pore geometry, solution openings) and were not caused by the injection process.

The model used in the study assumed that hydraulic characteristics related to flow and storage are defined as spatially continuous. This continuum assumption is appropriate for granular porous media. It may also be appropriate for fractured or solution-riddled media such as limestone if the density of the spatial distribution of solution features is sufficient that, on the scale of the hydrologic conditions modeled, hydrologic processes in the aquifer are similar to those of granular porous media. The existence of small-scale flow heterogeneities in limestone due to variations in channel tortuosity and cross-sectional area, and the resultant effect of mechanical mixing of two moving fluids at their interface, is one of the processes represented in the model as hydrodynamic dispersion.

It was considered beyond the scope of this study to assess recoverability in aquifers having characteristics that violate the continuum assumption, although it is possible that some results may apply. Flow in local sections of some limestone layers of south Florida might be

through large, discrete solution channels (conduits) or along bedding planes on a scale such that the continuum assumption is violated. In such a case, some physical processes (hydrodynamic dispersion) limiting recovery efficiency might be quite different from the processes the mathematical terms in the continuum model attempt to represent, so that predicted hydraulic and chemical responses might be incorrect.

DIGITAL MODELING TECHNIQUES

INTERA Deep Well Waste Disposal Model

A three-dimensional finite difference model for simulating flow and transport of solute and thermal energy resulting from injection of liquid waste (INTERCOMP Resource Development and Engineering, Inc., 1976; INTERA Environmental Consultants, Inc., 1979) was developed under sponsorship of the U.S. Geological Survey. The INTERA model has a variety of potential applications to variable-density solute-transport problems other than waste injection and was the principal tool of investigation used in this study. The model solves for the three independent variables—pressure, temperature, and solute fraction—in three-dimensional Cartesian coordinates, or in two-dimensional Cartesian coordinates for the representation of a prototype as a single (X-Y) layer or as a vertical (X-Z) slice. The solution may also be obtained in one- or two-dimensional cylindrical (R-Z) coordinates.

The nonlinear partial differential equation solved for the pressure field in three dimensions is

$$\frac{\partial}{\partial x}\left(\frac{\rho g k_x}{\mu}\frac{\partial p}{\partial x}\right)+\frac{\partial}{\partial y}\left(\frac{\rho g k_y}{\mu}\frac{\partial p}{\partial y}\right)+\frac{\partial}{\partial z}\left[\frac{\rho g k_z}{\mu}\left(\frac{\partial p}{\partial z}-\rho g\right)\right]=\rho g\Theta_0 C_r\frac{\partial p}{\partial t}+\Theta g\left(\rho_0 C_w\frac{\partial p}{\partial t}+\rho_0 C_T\frac{\partial T}{\partial t}+\frac{\partial \rho}{\partial C}\frac{\partial C}{\partial t}\right)+q' \quad (1)$$

where

ρ = $\rho(p,T,C)$ is density (M/L^3);
μ = $\mu(T,C)$ is dynamic viscosity (M/LT);
k_x, k_y, and k_z are intrinsic permeability in three coordinate directions alined with the principal axes of permeability (L^2);
p = $p(x,y,z,t)$ is pressure (M/LT^2);
g = gravitational acceleration (L/T^2);
Θ = $\Theta_0[1+C_r(p-p_0)]$ where Θ_0 is porosity (dimensionless) at some reference pressure p_0;
ρ_0 = density at reference conditions p_0, T_0, and C_0; and
$\frac{\partial \rho}{\partial C}$ = $\rho(p_1,T_1,C_1)-\rho(p_1,T_1,C_0)$ estimates the variation of density with solute fraction;

and where

P_1 and T_1 are some arbitrary conditions;
T = $T(x,y,z,t)$ is temperature (temperature units);
C = $C(x,y,z,t)$ concentration expressed as a unitless fraction where $C\epsilon\langle 0,1\rangle = \langle C_0,C_1\rangle$;
C_r = compressibility of the aquifer material (LT^2/M);
C_w = compressibility of water (LT^2/M);
C_T = coefficient of thermal expansion (reciprocal temperature units); and
q = sum of sources and sinks of fluid, expressed as mass flux per unit volume (M/L^3T).

Aquifer storativity is described by inputs of porosity, layer thickness, density, and compressibilities of water and of the aquifer material. Permeability is described by spatial distributions of hydraulic conductivity values at specified conditions of pressure, temperature, and concentration fraction.

The effect of injection and withdrawal stresses on the pressure field is entered in the solution equation as the q' term. All other terms on the right-hand side of the equation constitute the change in storage term. The functional dependence of fluid density and viscosity on changes of pressure, temperature, and concentration is incorporated into the model computations. The hydraulic conductivity values are also corrected whenever fluid properties change with time. The terms on the left-hand side of the equation representing net advective motion of fluid take into account the effects of spatial density gradients.

The INTERA model equation for solute transport is similar to the one derived by Konikow and Grove (1977). Using the summation convention for convenience, and letting X_i ($i=1, 2, 3$) denote the three Cartesian coordinates (x, y, z), it is written

$$\frac{\partial}{\partial x_i}\left(\frac{C\rho g k_{ii}}{\mu}\frac{\partial p}{\partial x_i}\right)+\frac{\partial}{\partial x_i}\left(\rho g E_{ij}\frac{\partial C}{\partial x_j}\right)=C\rho g\Theta C_r\frac{\partial p}{\partial t}+\Theta g C\left(\rho_0 C_w\frac{\partial p}{\partial t}+\rho_0 C_T\frac{\partial T}{\partial t}+\frac{\partial \rho}{\partial C}\frac{\partial C}{\partial t}\right)+\rho g\Theta\frac{\partial C}{\partial t}+Cq+\Sigma C_i q_i . \quad (2)$$

Terms (E_{ij}) not defined for equation 1 are components of the dispersion tensor (L^2/T):

$E_{ij} = E_{ij}(u, \alpha_l, \alpha_t, D_m)$, where u is fluid velocity (L/T), α_l, α_t are longitudinal and transverse dispersivities (L), and D_m is molecular diffusivity (L^2/T);

q = the sum of fluid sinks (M/L^3T); and

q_i = a source of fluid (M/L^3T) of concentration C_i.

Fractional values (C) describe the concentration of some water ($C = 1$) in a mixture with another water ($C = 0$). Either water may be considered to contain some actual or hypothetical solute. Any fluid influxes into the aquifer, including well injection, can be described as a mixture of the two waters. The two waters ($C = 0$ and $C = 1$) are assigned density values at specified temperature and pressure conditions, and this density contrast specifies a linear variation of density with concentration fraction. Values of C can also be considered to represent the concentration of a solute ranging linearly between the concentrations present in the two waters. $C = 1$ can refer to wastewater injected into a native aquifer fluid ($C = 0$) or to the concentration of some real or hypothetical tracer contined only in the injected wastewater. In this study, $C = 0$ referred to pure freshwater and $C = 1$ referred to the brackish or saline native aquifer water. Injected freshwater was assigned a concentration value slightly greater than 0 to represent its slight chloride concentration.

Other coefficients describe the thermal behavior of the fluid and the aquifer. Various constant-condition or dynamic boundary specifications describe fluxes of water, solute, and heat at the boundaries of the model grid. For the hypothetical simulation of transport in this study, it was considered satisfactory to specify constant conditions for pressure and solute fraction at boundaries far removed from the injected mass of freshwater. Temperature was assumed uniform throughout and along all boundaries, and the temperature equation (analogous to equation 2) was not solved.

The model equations for pressure, concentration, and temperature are approximated with finite difference techniques in which the aquifer is represented as a three-dimensional, variable, block-centered grid. The user may specify that the spatial derivative terms be approximated at the current (unknown) time level (implicit) or at the midpoint (centered in time) between previous (known) and current times (Crank-Nicholson). In addition, the advective terms may be spatially differenced by a backward or a centered scheme. The three equations for pressure, temperature, and concentration are decoupled with matrix operations and solved in the given sequence. The resultant systems of linear equations may be solved either by a direct method with special ordering (Price and Coats, 1973) or by line successive overrelaxation, an iterative method.

Modifications were made to the INTERA model to simulate repeated cycles of injection and recovery, to specify directional permeability changes with successive injection and withdrawal cycles, and to simulate the shutting down of withdrawal wells when withdrawn water exceeded a specified limit of chloride concentration.

Hydrodynamic Dispersion and Its Representation

Dispersion is the process whereby some of the injected fluid spreads beyond the spatial limits of its displacement volume while some of the resident fluid remains within these spatial limits. Well-defined bulk displacement does not occur because movement of fluid outward from the well is through a number of discrete pathways which vary in size and tortuosity, and flow varies within the cross section of each one. If a well were drilled near the approximate boundary between injected and native fluids, the many flow channels penetrated would contain waters of varying salinity. This mixing is termed "mechanical dispersion" and may be thought of in two ways: (1) the blend of injected and native water from turbulence or shear stress induced by flow, or (2) the adjacent location of pockets of water of contrasting chloride concentration induced by nonuniform flow. Which concept is more appropriate depends on the pore geometry of the aquifer material. The radial zone in which mixing occurs is referred to herein as the transition zone.

The dispersion terms of equation 2 are a continuum representation, the validity of which depends on the assumption that heterogeneities in flow speed and direction are sufficiently well distributed and small on the scale of the transport distances of the injected freshwater. If flow is through large conduits, as in highly cavernous zones, such a representation probably will not be valid.

The degree of dispersion parallel and perpendicular to the direction of flow is specified by a pair of coefficients—longitudinal (α_l) and transverse (α_t) dispersivity—, each specifying a linear parametric dependence on the velocity of flow (Scheidegger, 1961; Bear, 1972). In Cartesian coordinates, transverse dispersion occurs in the plane normal to the direction of flow. In a two-dimensional areal simulation, transverse dispersion is confined to the plane in which flow occurs (lateral transverse dispersion). Estimates of longitudinal dispersivity in field situations have been given by Reeder and others (1976) and also by Ehrlich and others (1979).

In many subsequent analyses done in cylindrical coordinates, flow about the wells in a layered system is radial, with a negligible vertical component, and adjacent layers have highly contrasting permeability and different flow rates. When this results in a salinity contrast between layers, the transverse dispersivity parameter (α_t) expresses the degree of dispersion that can occur vertically, across the boundary between layers. Interlayer dispersion is a term used herein to refer to this, and its usage is restricted to this type of flow regime.

Few data are available to determine whether an appreciable degree of interlayer dispersion actually occurs. The concept requires the definition of adjacent layers with uniform but contrasting hydraulic characteristics, which can only be a generalization of natural layering. A possible conceptual model of interlayer dispersion is that the orientation of pore spaces or solution channels could give flow near the interface a partly vertical orientation so that appreciable amounts of injected water cross this interface, even when vertical hydraulic gradients are insufficient to cause appreciable vertical flow. A transition zone would then develop about the interface between the layers because of heterogeneities in the paths of vertical fluid movement. Injected freshwater could then enter a less permeable layer from a permeable layer at radii not yet reached by radial flow of freshwater in the less permeable zone. Being perpendicular to the direction of flow, interlayer dispersion would probably be of lesser degree than dispersion in the direction of flow.

Figure 2 illustrates the concepts of dispersion in the direction of flow and between layers. Figure 2*A* depicts a broader (more diffuse) transition zone between injected and native waters in the more permeable layer in which radial flow velocity is greater. In the less permeable layer, the transition zone is narrower (sharper) and represents the mixing of a smaller volume of water than occurs in the more permeable layer of same thickness. Average chloride concentration increases continuously with radial distance in the transition zone. If the native water is not too saline, some water in the zone may be potable, but the amount is in inverse relation to the native water salinity. Figure 2*B* shows both dispersion in the direction of flow and interlayer dispersion in the case of two layers of contrasting permeability in which radial outflow from a well is taking place. This conceptual model is of a continuous transition zone across the two layers. Figure 2*C* is similar to 2*A*, except that the layer of higher permeability is thicker. The transition zone is narrower (sharper), vertically elongated, and nearer the well.

Reeder and others (1976) used an approximate formula, developed by Lau and others (1959), which describes the variation of concentration within the transition zone during radial outflow from a well in a uniform, isotropic aquifer of thickness h and porosity Θ:

$$C/C_0 = 1/2\ erfc\left[\frac{r-R}{(4/3\ \alpha_l R)^{1/2}}\right], \qquad (3)$$

where

erfc is the complementary error function;

C/C_0 is a unitless fraction having values ranging from 0 to 1 representing the concentration of native water at radius r;

R is defined by $V=\pi\Theta hR^2$, where V is the volume injected [R would be the radius of the cylindrical slug of injected water if there were no mixing at its boundary and is the radius of the volume centroid of the transition zone, where $C/C_0=0.50$] (L); and

α_l is longitudinal dispersivity (L).

It may be noted that C/C_0 is expressed as a function of position and volume (r and R), even though dispersion is understood to be a result of fluid motion. Equation 3 also shows the zone to become broader at larger radii (R). Suppose C/C_0 values of 0.16 and 0.84 are arbitrarily chosen to delimit the transition zone at radii $r_{0.16}$ and $r_{0.84}$ and it is assumed that no interlayer dispersion occurs (fig. 2*A*). From a table of values of the error function, it can be shown that:

$$R - r_{0.16} = r_{0.84} - R = AR^{1/2}, \qquad (4)$$

where $A = 0.7032\ (4/3\ \alpha_l)^{1/2}$.

An analytic relation with which to compare subsequent model-based recovery efficiency relations can now be stated showing that the ratio of the volume (V_{zf}) of the transition zone to the volume (V_{fw}) of freshwater ($C/C_0 < 0.16$) encircled by it depends on longitudinal dispersivity, aquifer geometry, and the volume injected:

$$\frac{V_{zf}}{V_{fw}} = \frac{\pi\Theta h(r_{0.84^2} - r_{0.16^2})}{\pi\Theta h r_{0.16^2}}$$

$$= \frac{4A}{R^{1/2} - 2A + A^2R^{-1/2}} \qquad (5)$$

$$= \frac{4A}{\left(\frac{V}{\pi\Theta h}\right)^{1/4} - 2A + A^2\left(\frac{V}{\pi\Theta h}\right)^{-1/4}}.$$

The INTERA model representation of dispersion is a somewhat simplified representation of a group of diverse and poorly understood processes. Current research seeks better ways to represent it and additional data to describe the physical processes it quantifies. The representation is analogous to the Fickian model for molecular diffusion and suggests that dispersion occurs as the transfer of solute in the direction of decreasing solute concentration. Alternatively, as encoded in the INTERA model, it could be regarded as the equal and opposite exchange of fluid between grid cells, with the fluid received by one cell having the fractional concentration (C) of the other cell. This is analogous to the concept that dispersion occurs during injection as the nonuniform bulk displacement of saline water by freshwater. If interlayer dispersive flux occurs, this might cause complex hydraulic interaction between

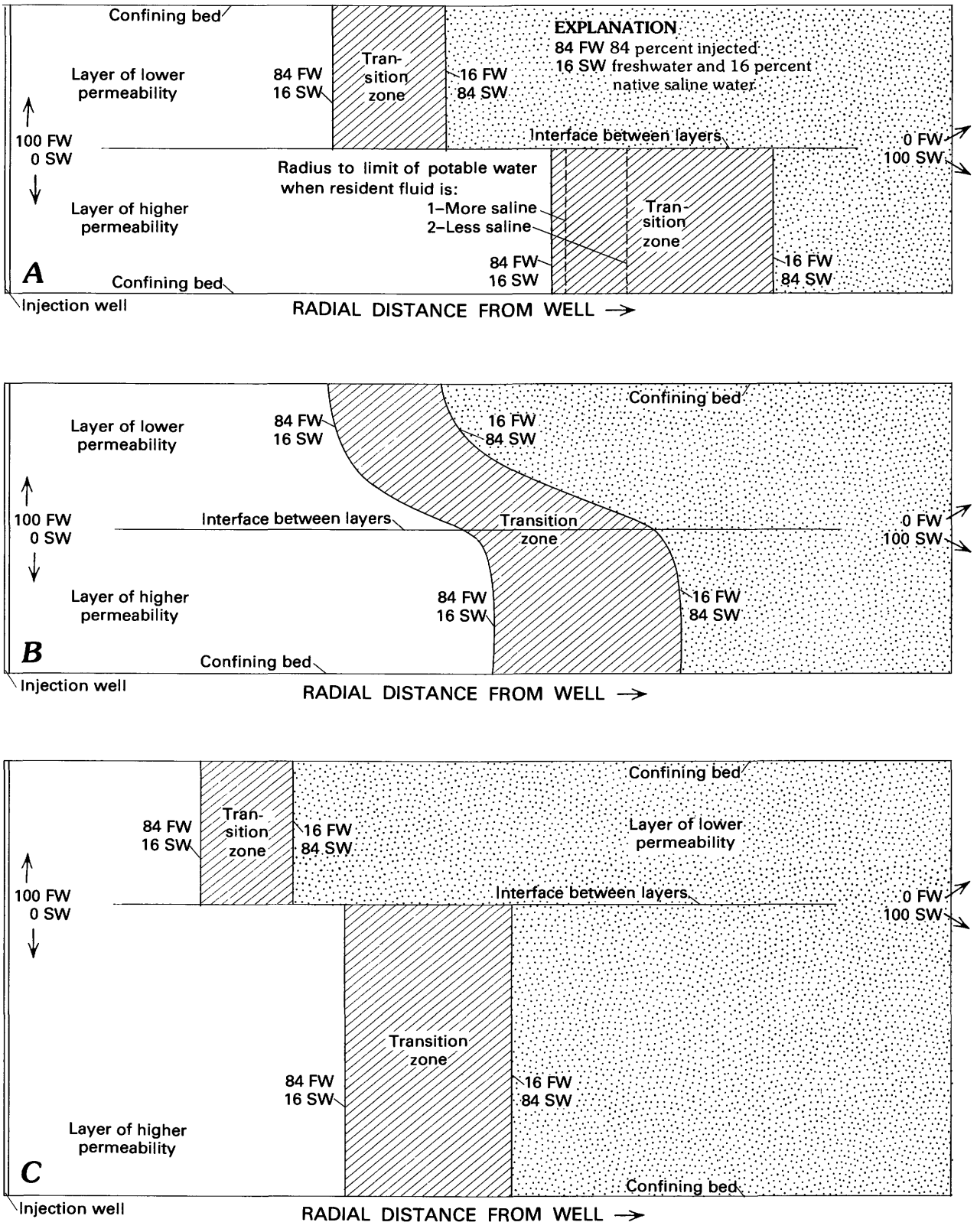

Figure 2. Conceptual models of dispersion in the direction of flow and between layers. Cases shown are: *A*—adjacent layers of higher and lower permeability, no interlayer dispersion; *B*—same as case *A*, but interlayer dispersion occurs; and *C*—same as case *A*, except that the layer of higher permeability is thicker.

layers, but the INTERA representation as the exchange of waters of different concentration would merely modify water density in the layers.

In subsequent sections, results of certain analyses are indicated to be particularly dependent on the ability of the Fickian diffusion model to represent adequately the complex processes of mixing and uneven flow referred to as hydrodynamic dispersion. Interpretations based on the indicated analyses could be incorrect if the representation fails in the context of those particular analyses.

Lateral transverse dispersion most likely is unimportant in radially symmetric flow. Model computations of radial flow in a planar Cartesian grid system with and without the specification of a significant level of lateral transverse dispersion showed very little difference.

The hydrodynamic dispersion terms in equation 2 also include molecular diffusion, which in field situations of fluids moving at an appreciable speed is usually considered to be of negligible magnitude compared with mechanical dispersion (Reeder and others, 1976). Literature values for molecular diffusion range from 0.1 ft²/d (Hoopes and Harleman, 1967) to 1×10^{-5} ft²/d (INTERCOMP Resource Development and Engineering, 1976). If longitudinal dispersivity were 4 ft, a fluid particle velocity of at least 0.25 ft/d would ensure that mechanical dispersion, approximated as $\alpha_l \cdot v = 4$ ft·0.25 ft/d = 1 ft²/d, was at least one order of magnitude greater than either estimate of molecular diffusion.

The effect of the molecular diffusion component on the transition zone can also be estimated using the equation of Hoopes and Harleman (1967):

$$C/C_0 = \frac{1}{2}\, erfc\left[\left(\frac{r^2}{2} - \frac{R^2}{2}\right) \Big/ \left(\frac{4}{3}\alpha_l r^3 + \frac{2\pi h\Theta}{Q} D_m r^4\right)^{1/2}\right]. \quad (6)$$

This is a more precise form of equation 3 and takes molecular diffusion (D_m) into account. If the 50 percent concentration radius (R) is 300 ft, the layer thickness (h) is 12 ft, porosity (Θ) is 0.35, the injection (withdrawal) rate (Q) is 100,000 ft³/d, and the molecular diffusion rate (D_m) is zero, the concentration (C/C_0) at 325 ft is about 0.21 when $\alpha_l = 4$ ft and about 0.38 when $\alpha_l = 30$ ft. At 350 ft, the concentration is about 0.06 when $\alpha_l = 4$ ft and about 0.29 when $\alpha_l = 30$ ft. When $D_m = 0.1$ ft²/d and $\alpha_l = 4$ ft, the argument of the error function (*erf*) changes by 5.4×10^{-4} at 325 ft and by 9.3×10^{-4} at 350 ft. When $\alpha_l = 30$ ft, the argument changes by 0.26×10^{-4} at 325 ft and by 0.45×10^{-4} at 350 ft. The differences in computed concentration are negligible (less than 0.0015). If D_m were 1×10^{-5} ft²/d, the computed changes would be infinitesimal.

Computational Problems

Computational stability problems are inherent in the various optional differencing techniques. The backward differencing scheme has the drawback of greatly increasing the level of "numerical dispersion," that is, the method itself broadens the simulated transition zone. Numerical dispersion and the mathematical representation of hydrodynamic dispersion are indistinguishable in the computed results. Theoretical discussions of numerical dispersion have been published by Lantz (1971) and by Pinder and Gray (1977). Time-step lengths and grid-block sizes must be kept small if this numerical error is to be negligible compared with the magnitude of the physical dispersion (INTERCOMP Resource Development and Engineering, Inc., 1976). It is not economically feasible to meet these requirements when simulating a problem of moderately large time and spatial scales. The grid-size and time-step compromises requires to stay within budget and computer memory limits can severely distort the solution.

One of the primary objectives of the modeling effort was to compute the fraction of solute contained in the composite water mixture withdrawn during recovery from multiple layers of varying solute concentration. This depended on the degree of dispersive mixing about the interface during injection and withdrawal. Thus, any numerical error appreciably increasing the apparent level of dispersion would have made the results unrepresentative of the physical situation. For this reason, and given the time and spatial scale limitations of the simulations, backward differencing schemes could not be used.

Central differencing schemes tend to introduce spatial or temporal oscillations. Spatial oscillations are most evident near the interface between injected and resident fluids. If values of 0.0 and 1.0 represent freshwater and the resident brackish water, respectively, values less than 0.0 just inside the freshwater and values greater than 1.0 just inside the resident water ("undershoot" and "overshoot") are sometimes computed. This is discussed theoretically by Price and others (1966) and by Pinder and Gray (1977). Discretization criteria used to minimize oscillation are given by INTERCOMP Resource Development and Engineering, Inc. (1976), and consist of block size and time step size restrictions related to the estimated level of physical dispersion. These rules are not as restrictive as the ones required to prevent numerical dispersion, but if greatly violated, the computed results can be too distorted for interpretation.

In this study, it was possible to choose relatively economical spatial and time discretizations sufficiently meeting the restrictions of the central differencing method so as to prevent severe oscillations. The lesser oscillations that occurred were, nevertheless, of concern, and many changes of grid design were made to optimize solution stability. One undesirable solution behavior

affecting the planar Cartesian (X–Y) simulation of injection and withdrawal from a single well was row or column oscillation. All values for entire rows (or columns) between opposite boundaries showed a pattern of a spatial oscillation with respect to the values of adjacent rows.

The major concern in model runs was the distortion caused by spatial oscillations as the interface returned to the well during withdrawal. However, results showed oscillations diminishing and a realistic progression of increasing concentration values at the well as the last freshwater was withdrawn. The correspondence of low dispersion levels and oscillatory behavior indicated that it was not economically possible to simulate sharp fronts in large-scale problems, as this required a very fine grid mesh in all locations of interface movement, making the resulting solution matrix very large.

Design of Prototype Aquifer

The Hialeah site injection zone was used as a basis for the design of a prototype aquifer for model tests. Hydraulic and chemical parameters describing this zone (fig. 3) were estimated by F. W. Meyer (oral commun., 1980) on the basis of geophysical logs from the injection well and the single observation well. Velocity logs, run during injection and withdrawal regimes, delineated flow zones by showing depth intervals where augmentation of flow occurred. The logs were correlated with conductivity and temperature logs, which showed depths at which occurred appreciable contribution of flow of different temperature and salinity than that of flow from underlying zones. The layering depicted in figure 3 is considered rather generalized because of the limited precision with which the logs showed changes. Layers 3 and 4 generally correspond to the most permeable part of the zone and were grouped as one layer in many analyses made with the cylindrical-coordinates version of the INTERA model. The two layerings are referred to in later text as the six-layer (layers 3 and 4 separate) and five-layer (layers 3 and 4 combined) radial models.

Vertical salinity heterogeneities at Hialeah were considered to unnecessarily complicate sensitivity tests made with the radial model for the purpose of evaluating relations in a hypothetical prototype only generally representative of the actual injection zone. Therefore, the prototype was simplified with the assumption of a vertically uniform initial chloride distribution, represented in the model by a resident fluid density value (ρ_{res}). Some values used were (1) 62.50 lb/ft^3, representing the multilayer, composite background water samples collected at Hialeah (1,200–1,300 mg/L of chloride), (2) 62.57 lb/ft^3, representing the most saline layer at the site (about 2,000 mg/L of chloride), (3) 63.07 lb/ft^3, an arbitrary value representing water somewhat more saline than the injection zone (perhaps 7,000–8,000 mg/L of chloride), and (4) 64.00 lb/ft^3, representing seawater (19,000 mg/L of chloride). The density of the injected freshwater (ρ_{inj}) was entered as slightly greater than pure freshwater (62.4 lb/ft^3; $C=0$), similar to the 65 mg/L chloride water injected in the first Hialeah test.

Injection and withdrawal rates (Q_i and Q_w) used in most radial analyses were the average rates of the first Hialeah injection tests, 105,661 ft^3/d and 62,047 ft^3/d. The length of the injection period in most analyses was that of the first Hialeah injection (53 days), and withdrawal was assumed to end when the increasingly saline recovered water exceeded the maximum chloride level (250 mg/L) deemed acceptable for potability.

The prototype aquifer for areal simulations was the 12-foot-thick most permeable layer, and the injection rate was 65 percent of the Hialeah injection test inflow rate, the proportion of total flow assumed to occur within the most permeable layer.

Because of the lack of data showing the degree of dispersion, three standard dispersion models (sets of parameter values representing some hypothetical degree of dispersion) were chosen for radial analyses and were supplemented by additional models as needed. The parameter values were longitudinal dispersivity (α_l) and transverse dispersivity (α_t):

Dispersion model	α_l *(ft)*	α_t *(ft)*
1	4	0
2	4	1
3	30	10

Dispersion model 1 is a low degree of dispersion in the radial flow direction and no interlayer dispersion. Model 2 introduces a moderate degree of interlayer dispersion, and model 3 represents appreciable degrees of dispersion in the radial flow direction and between layers. The longitudinal dispersivity value of model 3 has some support, in that Ehrlich and others (1979), with the collaboration of Ren Jen Sun (written commun., 1978), estimated a value of about 30 ft at a waste injection site near Pensacola, Fla. In areal analyses, longitudinal dispersivity (in the direction of flow) was generally 4 ft. Because of the radial symmetry of the flow field, lateral transverse dispersivity (α_t) (perpendicular to the direction of flow) had little effect and was generally set at 0.

The selected value for rock compressibility, 6×10^{-6} in.^{2}/lb, was comparable to the value of 4×10^{-6} in.^{2}/lb used in model verification tests (INTERCOMP Resource Development and Engineering, 1976).

In both radial and areal analyses, pressure was considered initially uniform either radially or areally. Constant boundary pressure conditions were specified at a large distance (30,000 ft) from the hypothetical injection

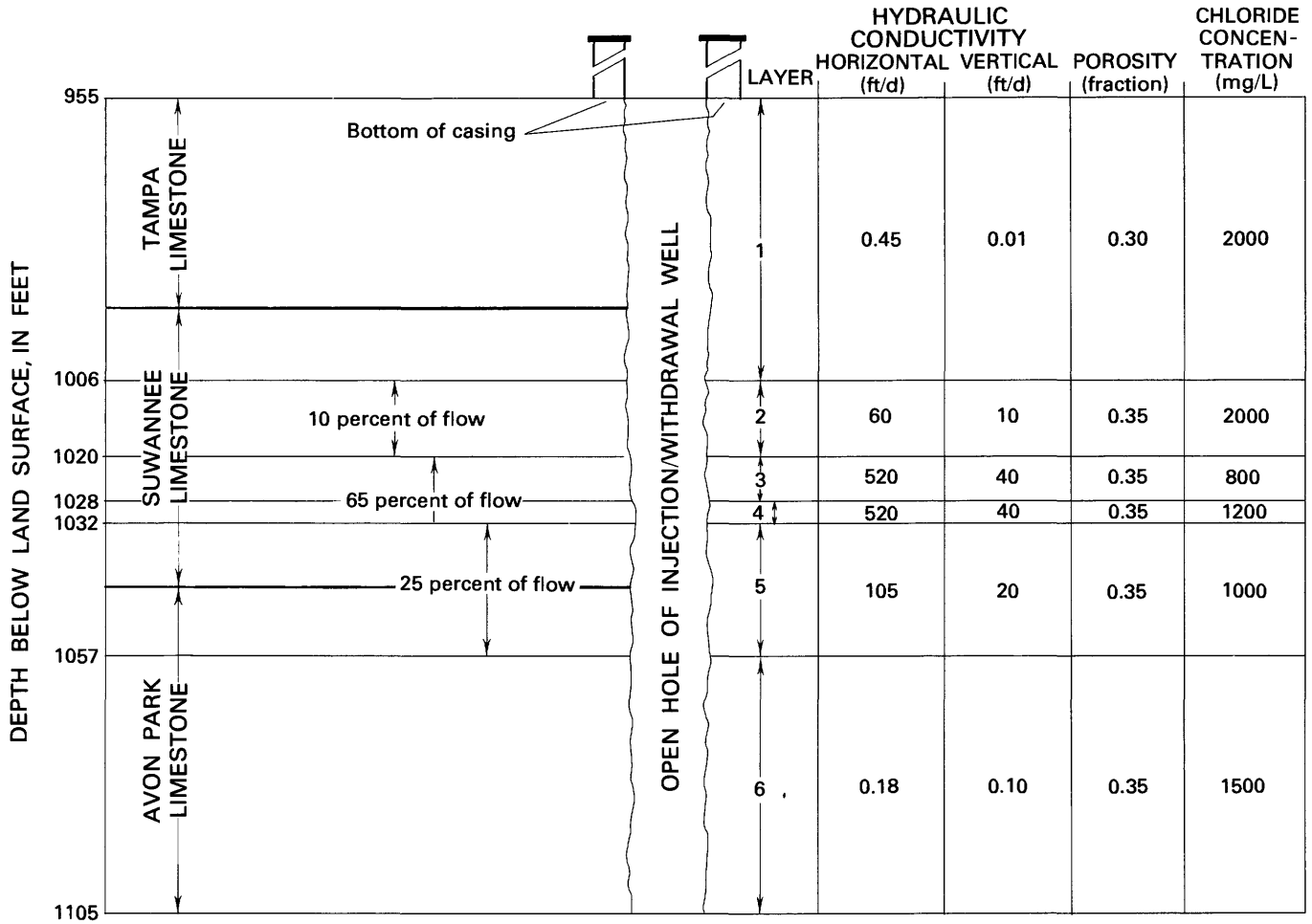

Figure 3. Prototype aquifer resembling the Tertiary Limestone injection zone at the Hialeah test site, Dade County, Fla. Hydraulic and water-quality parameter estimates are generally based on analyses of Hialeah test data by F. W. Meyer (oral commun., 1980).

wells and were equal to the uniform values. The error in pressure near the well resulting from the constant boundary assumption was insignificant and could not affect the simulation of flow of injected freshwater, as this was controlled by constant-rate specifications for inflow and outflow. Constant boundary specifications for chloride concentration (far from radii reached by injected freshwater) were the same as the concentrations assumed as initial conditions.

DEPENDENCE OF FRESHWATER RECOVERY ON HYDROGEOLOGIC CHARACTERISTICS

Aquifer Permeability and Buoyancy Stratification

The permeability of the aquifer material determines the volumetric rate of injection or withdrawal impelled by a given wellhead pressure, or the pressure gradient in the aquifer that must be maintained to inject or withdraw water at a chosen rate. Because the permeabilities of limestone aquifers underlying south Florida vary greatly, a knowledge of the relation between permeability and the recoverability of injected freshwater would provide useful guidance in feasibility decisions involving a tradeoff between required wellhead pressures and recovery losses.

Aquifer permeability affects recovery through the process of buoyancy stratification. When fluids of different densities interface, gravitational force combined with the deformability of fluids causes the less dense fluid to rise and flow over the more dense fluid. The magnitude of this effect depends primarily on the relative densities and the permeability.

If a significant amount of injected freshwater buoys upward about the injection and withdrawal well, the amount that is recoverable will be affected. Buoyancy causes saltwater to migrate in toward the bottom of the well and freshwater to migrate outward in upper intervals. During withdrawal, saltwater reaches the bottom of the well, contaminating the composite of water with-

drawn from the entire well, even while freshwater remains in the upper part of the injection zone. A theoretical analysis of buoyancy stratification was described by Kimbler and others (1975), but their physical model was not designed to provide experimental verification.

In hydraulic flow models, permeability is usually lumped with fluid properties and specified as the hydraulic conductivity parameter. If the principal components of permeability are alined with the radial and vertical axes of cylindrical coordinates, hydraulic conductivity is specified by a pair of coefficients, radial hydraulic conductivity (k_r) and vertical hydraulic conductivity (k_z). An assumption inherent in the INTERA model and carried over into the analyses in this study is that there is no correlation between hydraulic conductivity and hydrodynamic dispersion. This meant that conductivity estimates were increased or decreased independently of any changes in the specified levels of dispersion.

No quantitative relation between recoverability and wellhead pressure will be developed, as this would depend on the choice of injection rate, the design of the well, and the extent of well-bore plugging.

Methodology of Analysis

The purpose of the first series of computations was to establish qualitative and quantitative relations with recovery efficiency. The computations were done using the five-layer radial model with an initially uniform resident fluid density of 62.57 lb/ft^3. Dispersion model 1 was used. In one computation, lateral hydraulic conductivity values were increased by a factor of 100 to assess the effect on recovery of a very high level of lateral permeability. In other computations, both lateral and vertical permeability values were changed by a common factor which ranged from 0.5 to 100 to establish a quantitative relation. In a similar series of computations, it was assumed that resident fluid was of seawater density (64.0 lb/ft^3).

A subsequent series of computations provided a more detailed portrayal of buoyancy stratification occurring during injection and withdrawal than could be shown by the crude vertical discretization of the five- and six-layer representations. This helped to show the distribution and movement of injected freshwater during and after injection and withdrawal. A prototype aquifer different from that used in other analyses was designed. The cylindrical-coordinates version of the INTERA model was used for this simulation of 17 layers, each 10 ft thick and having the same aquifer characteristics. The top layer was represented as fully confined from above. Porosity was specified to be 35 percent. Spatially uniform horizontal and vertical hydraulic conductivities and resident fluid salinity were varied to observe buoyancy effects. Radial discretization was into 27 annuli, and the injection well was represented as fully penetrating. The three standard dispersion models were augmented by a fourth ($\alpha_l = 30$ ft and $\alpha_t = 0$) to help distinguish between the effects of dispersion in the direction of flow and interlayer dispersion. Computer processing charges for the 17-layer simulations were appreciable, which explains why they were not used to establish quantitative relations.

In a real well with 170 ft of open hole, head losses would occur with depth because of friction and the decrease of flow. In this idealized portrayal of buoyancy stratification, these and other processes related to well construction and operation were ignored.

Results of Analysis

The purpose of the initial computations was to determine whether buoyancy stratification occurred in highly permeable aquifers and if recovery efficiency was affected. Control for the sensitivity tests was the five-layer simulation using a resident fluid density value of 62.57 lb/ft^3 and the Hialeah site hydraulic conductivity estimates, for which recovery efficiency was about 67 percent. After 53 days of simulated injection, the radial distance to the 50 percent concentration in layer 2 was 168 ft and in layer 4 was 222 ft. The 50 percent radius in the intervening most permeable layer, layer 3, was much greater (507 ft). In the first test for buoyancy, all lateral hydraulic conductivities were increased a hundredfold from the values shown in figure 3. Results showed significant buoyancy stratification. After 53 days of simulated injection, 50 percent radii in layers 2 and 4 were 183 ft and 203 ft. Stratification continued during withdrawal, and recovery efficiency dropped to 55 percent. When vertical hydraulic conductivities were also increased by a factor of 200, buoyancy stratification became even more pronounced. Simulated freshwater radii in layers 2 and 4 at the end of injection were 294 ft and 181 ft, and recovery efficiency dropped to 22 percent. Results demonstrated that high lateral permeability alone promotes buoyancy, that high vertical permeability increases buoyancy, and that a reduction of recovery efficiency results.

Results of the computations to establish a quantitative relation by changing radial and vertical hydraulic conductivities (k_r and k_z) by the sample multiple (resident fluid density of 62.57 lb/ft^3) are as follows:

k_r *and* k_z *multiplied by*	*Recovery efficiency (percent)*
0.5	67.5
1.0	67.0
2.0	65.2
5.0	63.8
10.0	58.8
20.0	47.4
50.0	30.4
100.0	21.9

The small variation in recovery efficiency when Hialeah conductivities were doubled or halved indicated that for density contrasts and hydraulic conductivity estimates the same order of magnitude as at Hialeah, significant buoyancy stratification did not occur, and recoverability was not affected. The major change indicated in these tests was the wellhead pressure required at the specified pumping rate. Buoyancy stratification began to have a significant effect at horizontal and vertical hydraulic conductivity levels about 10 times the Hialeah values.

When the resident fluid was assumed to be of seawater salinity (density of 64 lb/ft^3) in the second series of tests, the buoyancy effect was more pronounced at lower values of hydraulic conductivity. The density of the Hialeah site resident water was 0.3 percent greater than that of the injected water, but seawater density was 2.6 percent greater. The following table lists the recovery efficiencies when lateral and vertical hydraulic conductivities were changed by the same factor from the nominal Hialeah values:

k_r *and* k_z *multiplied by*	*Recovery efficiency (percent)*
0.1	47.8
0.2	47.3
0.5	45.4
1.0	32.7
2.0	23.8
5.0	9.0

When Hialeah conductivity estimates were used, recovery efficiency was almost a third less than if the conductivities were one-tenth as high, and the difference was attributable to buoyancy stratification. The small difference between the recovery efficiency corresponding to one-tenth and one-fifth the Hialeah site conductivities indicates that little stratification occurred at these levels.

The following table presents a summary of results of tests with the 17-layer model:

Run	Resident fluid density (lb/ft^3)	Dispersivity (feet)	Hydraulic conductivity (ft/d)	Top and bottom 50 pct. radii separation (feet)	Recovery efficiency (pct.)
1, 2	62.5	Models 1, 2	k_r= 10.0 k_z= 10	3.5	---
3	64.0	Model 1	k_r= 100 k_z= 10	39.5	43.9
4, 5	64.0	Model 3 (run 5) and α_l=30, α_t=0 (run 4)	k_r= 100 k_z= 10	14.0	—
6	64.0	Model 1	k_r= 10,000 k_r= 10	133.0	26.7
7	64.0	Model 1	k_r= 10,000 k_z= 1,000	467.0	0.02

Interpolating between values at adjacent radial nodes was necessary to locate the radius of the 50 percent concentration mix of injected and resident fluids. Run 1 showed that after 53 days of injection, the 50 percent radius in the bottom layer was 3.5 ft closer to the well than in the top layer, 160 ft above. This slight inward migration of saltwater in the bottom layer would have negligible effect on recovery and is consistent with results of the recovery efficiency tests with the five-layer model in demonstrating that, for density contrasts, hydraulic conductivities, and permeable layer thicknesses comparable to those at the Hialeah site, the effect of freshwater buoyancy was negligible.

A degree of interlayer dispersion was introduced in run 2. Results were little different from those of run 1 and indicated that interlayer dispersion in the small lateral interval containing the nearly vertical fluid interface had no effect on buoyancy.

Run 3 was similar to run 1 except that the resident fluid had the density of seawater. The 50 percent radius in the bottom layer was 39.5 ft closer to the well than in the top layer, indicating appreciable inward migration of saline water in the lowest layer at conductivity levels comparable to those at the Hialeah site. This supports the result of the five-layer model test, which showed reduced recovery efficiency under these conditions.

Longitudinal dispersivity was increased to 30 ft in run 4, and the difference between the 50 percent radii in the top and bottom layers decreased to 14 ft. This indicates that higher dispersion in the direction of flow lessens the degree of simulated buoyancy stratification. Increasing the level of interlayer dispersion in run 5 did not affect the degree of buoyancy.

Results of run 6 show that at the end of 53 days of injection, the 50 percent concentration radius was located about 233 ft from the well in the top 10-ft layer. In contrast, in the adjacent layer, the 50 percent radius was located only about 167 ft from the well. In the lowest layer, it was located about 100 ft from the well. In most intervening layers, the radius was about 163 ft. A vertical fluid particle velocity of about 0.86 ft/d was computed in the freshwater region about the well, indicating that freshwater injected on the first day could buoy upward about 45 ft in 53 days. Run 6, incorporating the high value of lateral hydraulic conductivity, provided a vivid illustration (fig. 4) of the upward movement of freshwater, the depletion of freshwater at large radii in the lowermost layer, and the accumulation of freshwater at large radii in the uppermost layer. Intervening layers were relatively uniform in volumes of freshwater, as relatively uniform upward movement of water through those layers was portrayed. The substantial increase in buoyant flow above that computed in run 3 was caused solely by the hundredfold increase in lateral conductivity values, as the vertical conductivity values remained unchanged.

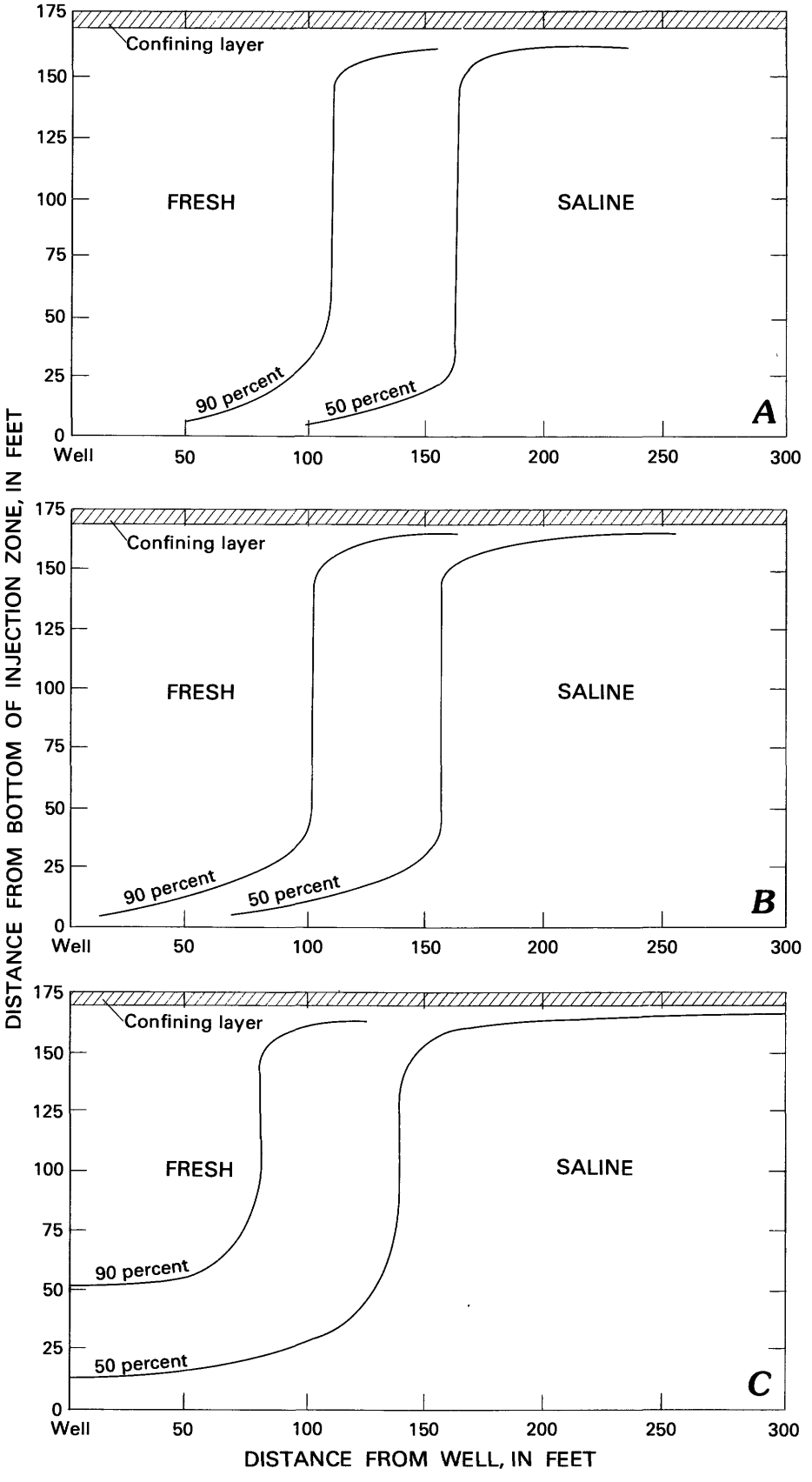
Confining layer
FRESH
SALINE
90 percent
50 percent
A
B
C
175
150
125
100
75
50
25
0
Well
50
100
150
200
250
300
DISTANCE FROM BOTTOM OF INJECTION ZONE, IN FEET
DISTANCE FROM WELL, IN FEET

Simulated recovery of injected water in run 6 showed continued vertical movement of freshwater and more rapid saline water inflow into the lower layers, causing early salinization of the water withdrawn from the lower part of the well. After 24 days of withdrawal, the multilevel composite of water withdrawn from the well was too saline to be potable, although considerable potable water was shown to remain about the well in upper layers (fig. 4*C*). The amount of potable water recovered at this time was 26.7 percent of that injected. This compared with a recovery efficiency of 43.9 percent for run 3 when lateral hydraulic conductivity values were lower.

In run 7, values of vertical hydraulic conductivity were also increased a hundredfold. Numerical results were considered reasonably accurate, though the computation was affected by numerical instability. Rapid vertical movement of injected freshwater occurred. The 50 percent concentration radius in the uppermost layer after 53 days of injection was about 473 ft, and that of the two lowest layers about 6 to 8 ft. The transition zone was broad in the upper and lower layers. Vertical particle velocity was computed to be about 22 ft/d in the freshwater region about the well. After about one-half hour of recovery, the multilevel composite of water from the well was too saline to be potable.

In summary, when aquifer characteristics were similar to those of the Hialeah site, buoyancy stratification in simulations was insignificant for water densities comparable to those at the Hialeah site but appreciable when the resident fluid was of seawater density. Dispersion in the direction of flow was a significant influence, but interlayer dispersion was not. When lateral hydraulic conductivities were much higher but vertical conductivities were low, and when the resident fluid was of seawater density, buoyancy stratification occurred to a major degree and recovery of freshwater was significantly reduced. When vertical hydraulic conductivities were also very high, vertical movement of freshwater virtually depleted lower layers, and recovery was negligible.

This latter result has special significance for water management in south Florida because the "boulder zone," a cavity-riddled dolomitic section of the Eocene Oldsmar Formation, contains water chemically very similar to seawater, and its hydraulic conductivity has been estimated to be on the order of 10^5 ft/d. Injected freshwater would buoy rapidly.

Figure 4. Vertical and radial distribution of freshwater resulting from buoyancy stratification during injection and withdrawal. Lines of 90 percent and 50 percent concentrations of injected freshwater are shown at: *A*—53 days, immediately after end of injection phase; *B*—60 days, after 7 days of withdrawal; and *C*—77 days, after 24 days of withdrawal, when multilayer composite chloride concentration reached 250 milligrams per liter (considered nonpotable).

Evidently, for every resident fluid density, there are levels of lateral and vertical hydraulic conductivity above which recovery efficiency is significantly reduced by buoyancy stratification. Cyclic injection becomes less productive, even as it becomes less costly because lower pressures are required to drive inflow and outflow. Because of the variability of permeability and native water density in limestone aquifers, the possibility of buoyancy must be evaluated on a site-specific basis.

Anisotropic Permeability

Permeability in the fractured and cavity-riddled limestone aquifers of south Florida may be anisotropic within the plane of flow (F. W. Meyer, oral commun., 1980). Model sensitivity tests were made to study the effect of anisotropy on recovery of injected freshwater. An assumption of the tests was that flow, though anisotropic, satisfied uniformity assumptions on the scale of the volume of water injected. This meant that the anisotropy did not correspond to discrete flow paths (conduits) as might occur in cavernous zones. It is unknown whether this can actually characterize limestone aquifers in south Florida. Another assumption required by the INTERA model was that longitudinal and transverse dispersivity were isotropic parameters (the dependence of the degree of dispersion on velocity was independent of direction). However, the actual degree of dispersion would be greater in the preferred flow direction because of the greater speed and extent of flow and the higher value of longitudinal dispersivity.

Although actual anisotropy within the plane of flow might not exhibit symmetry, it was convenient to assume that the X- and Y-axes of coordinates corresponded to the principal components (k_x and k_y) of a two-dimensional lateral permeability tensor. Anisotropy was considered to be related solely to the pore geometry of the aquifer and not to be caused by the injection operations; that is, the degree of anisotropy was unaffected by well-bore plugging during injection or by improved circulation within the well during withdrawal. As injected water moved in greater volume along the axis with the larger permeability component, the freshwater mass had an elliptical shape at the end of the injection phase. Conversely, as the unequal permeability components were assumed to be the same during withdrawal as during injection, the return of the injected water to the well was more rapid along the preferred axis.

Methodology of Analysis

The two-dimensional, planar flow version of the INTERA model was used for comparison simulations of anisotropic and isotropic (radial) flow from a single injection well. A symmetric 27×27 grid was used in all

runs, but the uniform 100-foot internal grid spacing used in the anisotropic permeability runs was different from the variable internal grid mesh used in the control runs of isotropic radial flow. In the anisotropic flow simulations, the lateral hydraulic conductivity (k_x and k_y) values of 520 ft/d were multiplied by factors of 1.7937 and 0.2063, respectively, so that $k_y/k_x = 0.115$. It was found, in attempts to simulate the breakthrough curve of freshwater at the observation well in the Hialeah tests (F. W. Meyer, oral commun., 1980), that this ratio led to freshwater transport along the axis of lower permeability (the Y-axis) at a rate similar to that in the direction of the observation well.

Two sets of comparison runs were made, one set assuming $\alpha_l = 4$ ft to represent a relatively sharp transition zone between injected and resident fluids, and the other assuming $\alpha_l = 30$ ft to represent a relatively diffuse transition zone. Other parameter choices were the previously stated nominal set of values representing the Hialeah site most permeable zone (layers 3 and 4 from fig. 3). The planar flow simulations assumed confinement above and below.

Results of Analysis

In the symmetrically anisotropic case, areal pressure contours during injection are elliptical (fig. 5*A*), as is the areal cross section of the freshwater mass at the end of the injection phase (fig. 5*B*). For comparison, the circular freshwater mass of the same volume that results in the isotropic case is also shown, as is the diminished elliptical mass after 47 days of withdrawal. When a relatively sharp transition zone ($\alpha_l = 4$ ft) was simulated, isotropic and anisotropic recovery efficiencies were 61 percent and 74 percent. When the broader transition zone ($\alpha_l = 30$ ft) was simulated, isotropic and anisotropic recovery efficiencies were 35 percent and 36 percent. However, the anisotropic runs exhibited pronounced row-wise oscillation, particularly for $\alpha_l = 4$ ft, making results difficult to interpret. Considering the different grid design, no confidence was placed in the predictions of higher values of recovery efficiency for the anisotropic case, and the computational results for $\alpha_l = 30$ ft indicated about the same recovery efficiency in both cases.

As directional flow was determined by the same permeability anisotropy during injection and withdrawal, saline water, even though farther from the well along the X-axis than the Y-axis at the end of injection, might be expected to arrive at the well from both directions at about the same time during withdrawal. If so, little potable water would remain in storage after withdrawal ended, as in the isotropic case. However, the different width of the transition zone in the two coordinate directions caused by the different speeds of flow raised the possibility that, near the end of withdrawal, water drawn from some directions could be more saline than water from other directions. If this were the case, a slight amount of potable water might be left in the injection zone. An analysis of this possibility was not feasible because such minor effects were obscured by numerical oscillations in the computations.

Hydrodynamic Dispersion

Model sensitivity tests were designed to illustrate the variation of recovery efficiency given various degrees of dispersion in the direction of flow and interlayer dispersion (fig. 2). Complete recovery of the injected freshwater should result, in the absence of well-bore plugging, background hydraulic gradients, and buoyancy effects, if no dispersive mixing occurs during injection or withdrawal. This has never occurred in operational cyclic injection tests.

In the transition zone between injected freshwater and resident saline water caused by dispersion, the average chloride concentration of the mixture increases outwardly. The variety of processes lumped as dispersion continue during withdrawal, causing the transition zone to return to the well. Recovery of usable water ends when the mixture of water reaching the well contains too much native saline water for the mixture to be potable. At this time, some freshwater remains unrecoverable in the nonpotable mix in the injection zone. If the potability limit is less than half the difference between injected and resident water salinities, the volume of unrecoverable injected freshwater is greater than the volume of recovered resident saline water, and the volume of potable water recovered is less than the volume of freshwater injected. Interlayer dispersion, if it occurs, also can reduce the amount of recoverable potable water by dispersing some injected freshwater into adjacent, less permeable layers, where it may be unrecoverable.

That recovery efficiency decreases as dispersive mixing increases is confirmed mathematically by considering equation 4 for the ratio of the volume of the transition zone to the volume of unmixed freshwater. Differentiating with respect to longitudinal dispersivity (α_l),

$$\frac{d}{d\alpha_l}\left(\frac{V_{zf}}{V_{fw}}\right) = \frac{d}{dA}\left(\frac{V_{zf}}{V_{fw}}\right)\frac{dA}{d\alpha_l}$$

$$= \frac{4\,(R^{1/2} - A^2R^{-1/2})(0.713)}{(R^{1/2} - 2A + A^2R^{-1/2})^2}\left(\frac{1}{3\alpha_l}\right)^{1/2}. \qquad (7)$$

The derivative is positive when $R > A^2 = 0.68\alpha_l$, indicating that the relative volume of the transition zone increases when α_l increases. Equation 4 does not consider interlayer dispersion. The condition $R > 0.68\alpha_l$ simply

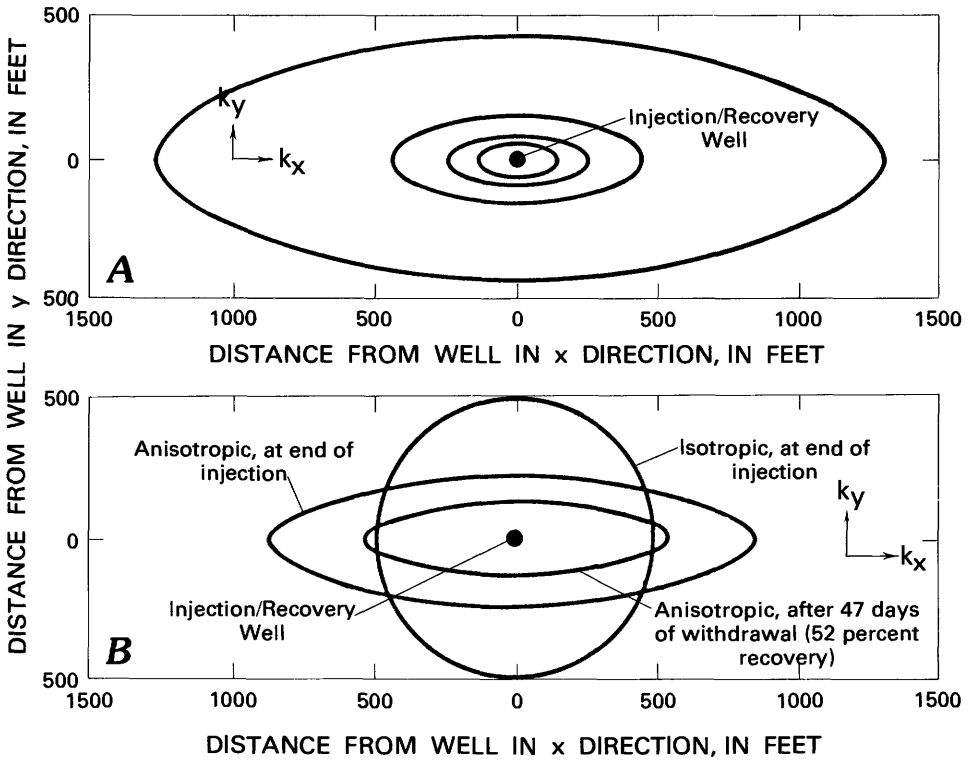

Figure 5. Lines of equal pressure and chloride concentration about the injection well when permeability is anisotropic. *A*—generalized lines of equal pressure during injection or withdrawal when permeability is anisotropic ($k_y/k_x = 0.115$); *B*—lines of 250 milligrams per liter chloride concentration when permeability is isotropic ($k_y/k_x = 1.0$) and when permeability is anisotropic ($k_y/k_x = 0.115$). (k_x and k_y are directional components of hydraulic conductivity.)

means that the volume of water injected must be great enough that the radius to the limit of freshwater is greater than a fraction of the dispersivity parameter. Ordinarily, the volume of injectant would be very much greater.

Methodology of Analysis

Few data were available to indicate the degree of dispersion in the direction of flow typical of saline limestone aquifers of south Florida, and no data were known to exist that could confirm the occurrence of interlayer dispersion or provide estimates of its degree. Sensitivity tests with the five-layer radial model were made with ranges of dispersivity values broad enough to show the relation to recovery efficiency, though it is possible that the actual degree of dispersion in an injection zone could be outside these ranges.

In the first series of tests, longitudinal dispersivity (α_l) was varied from 2 to 30 ft, and corresponding recovery efficiencies were computed. The conceptual significance of these dispersivity values is illustrated by considering the distances between the 84 percent and 16 percent freshwater concentrations within a transition zone centered at a radius of 289 ft from the injection well. These distances were estimated for each dispersivity value using the approximate formula of Reeder and others (1976). For a 2- to 30-foot range of values of α_l, the estimated distances ranged from 40 to 253 ft. It would have been desirable to also test values of longitudinal dispersivity less than 2 ft, representing even sharper transition zones, but the INTERA model computations became unstable in this range. Letting $\alpha_l = 0$ in this series of tests represented the assumption that no interlayer dispersion occurred.

A second series of tests was made in which the value of transverse dispersivity was varied from 0 to 2 ft. This procedure represented the variation of the degree of interlayer dispersion, because there was virtually no vertical component of flow. These values were all less than the value of 4 ft assigned to longitudinal dispersivity (α_l). Recovery efficiency was also computed for dispersion model 3, in which both longitudinal and transverse dispersivity values were larger (30 ft and 10 ft). The two series of comparison runs were made for the three previously cited resident fluid density values, 62.57, 63.07, and 64.00 lb/ft^3. The second value represented water with approximately 7,250 mg/L of chloride,

assuming dissolved solids and chloride concentrations to be in the same ratio as in seawater.

Results of Analysis

Figure 6 illustrates the variation of recovery efficiency in relation to longitudinal and transverse dispersivity values. Figure 6*A* shows the range of variation when transverse dispersivity was 0 (no interlayer dispersion) and longitudinal dispersivity was varied from 2 to 30 ft. Results portray the decrease in recovery of freshwater as the volume of the transition zone increases relative to the volume of uncontaminated freshwater about the well.

At the end of injection, the transition zone was broadest in the most permeable zone, a result of the greater velocity of radial flow in this zone. This remained the case as the transition zones in the various layers returned to the well during withdrawal. When the composite chloride concentration of withdrawn water reached the potability limit, the vertical distribution of chloride about the well bore was not vertically uniform. The most permeable layer contained the least saline, and still potable, water about the well bore, while less permeable zones contained saline water about the well bore. Useful recovery ended because the salinity of water contributed by less permeable layers was sufficiently high to make the composite saline, even though the contribution from the most permeable zone was still potable. Analyses of storage versus recovery relations and volume versus recovery relations showed similar effects. The physical reasonableness of this result depends on the adequacy of the mathematical representation of dispersion in the INTERA model. As previously stated, this is a rather indirect representation of a group of diverse and poorly understood processes.

Recovery efficiency varied inversely with transverse dispersivity (fig. 6*B*) at low ranges of the parameter. At higher ranges, recovery efficiency was unaffected by its variation. As transverse dispersivity increased, the corresponding increase in the degree of interlayer dispersion decreased the 50 percent concentration radius in the most permeable zone and increased it in adjacent zones as injected freshwater dispersed from the most permeable zone into adjacent zones (or as chloride was gained by freshwater in the most permeable zone, according to the INTERA model representation).

The five-layer radial model portrayed significant interlayer dispersion from the center layer into the second and fourth layers, but very little into the first or fifth layers because of the low radial flow velocities in those layers. A finer vertical discretization would have portrayed the interlayer dispersion in better detail, showing a gradual decrease in dispersive mixing with vertical distance from the most permeable layer.

When the increasing chloride concentration of the multilevel composite of withdrawn water reached the limit of potability, water in the most permeable layer was saline, while water in adjacent, less permeable layers remained potable, the reverse of what occurred in the case of no interlayer dispersion. The effect lessened with higher values of transverse dispersivity, apparently because the model simulated dispersion of freshwater from the less permeable layers back into the increasingly saline most permeable layer near the end of withdrawal.

Resident Fluid Salinity

In the transition zone surrounding the injected freshwater, salinity grades from that of the injected water to that of the saline resident water. The potable volume within the transition zone will depend on the salinity of the resident water. The higher this salinity, the greater is the range of salinity across the zone, and a smaller proportion of its water is within the potability limit. (This concept is illustrated in figure 2*A*.) Thus, recovery efficiency and resident water salinity are inversely related. An additional process limiting recovery efficiency at higher levels of resident fluid salinity is buoyancy stratification. No attempt was made to separate the effect of the two processes in these model sensitivity tests.

The significance of the recovery efficiency versus resident fluid density relation lies in the fact that the chloride concentration of permeable aquifers in south Florida may vary from slightly brackish, as in the injection zone at the Hialeah test site (800 to 2,000 mg/L of chloride), to seawater salinity (19,000 mg/L chloride), as in the deep "boulder zone." A consideration of the degree to which the salinity of the resident water limits recovery will help guide decisions concerning the feasibility of subsurface freshwater storage at specific sites.

Methodology of Analysis

The series of model-sensitivity tests used to define the relation between recovery efficiency and hydrodynamic dispersion were also used to define the salinity relations. The three previously cited resident fluid densities, 62.57, 63.07, and 64.00 lb/ft^3, were used for the comparisons by specifying them as vertically uniform initial conditions. Relations were established for a range of longitudinal and vertical dispersivity combinations.

Results of Analysis

Figure 7 shows the decline of recovery efficiency with increasing resident water salinity for the various dispersivity combinations as computed using the INTERA

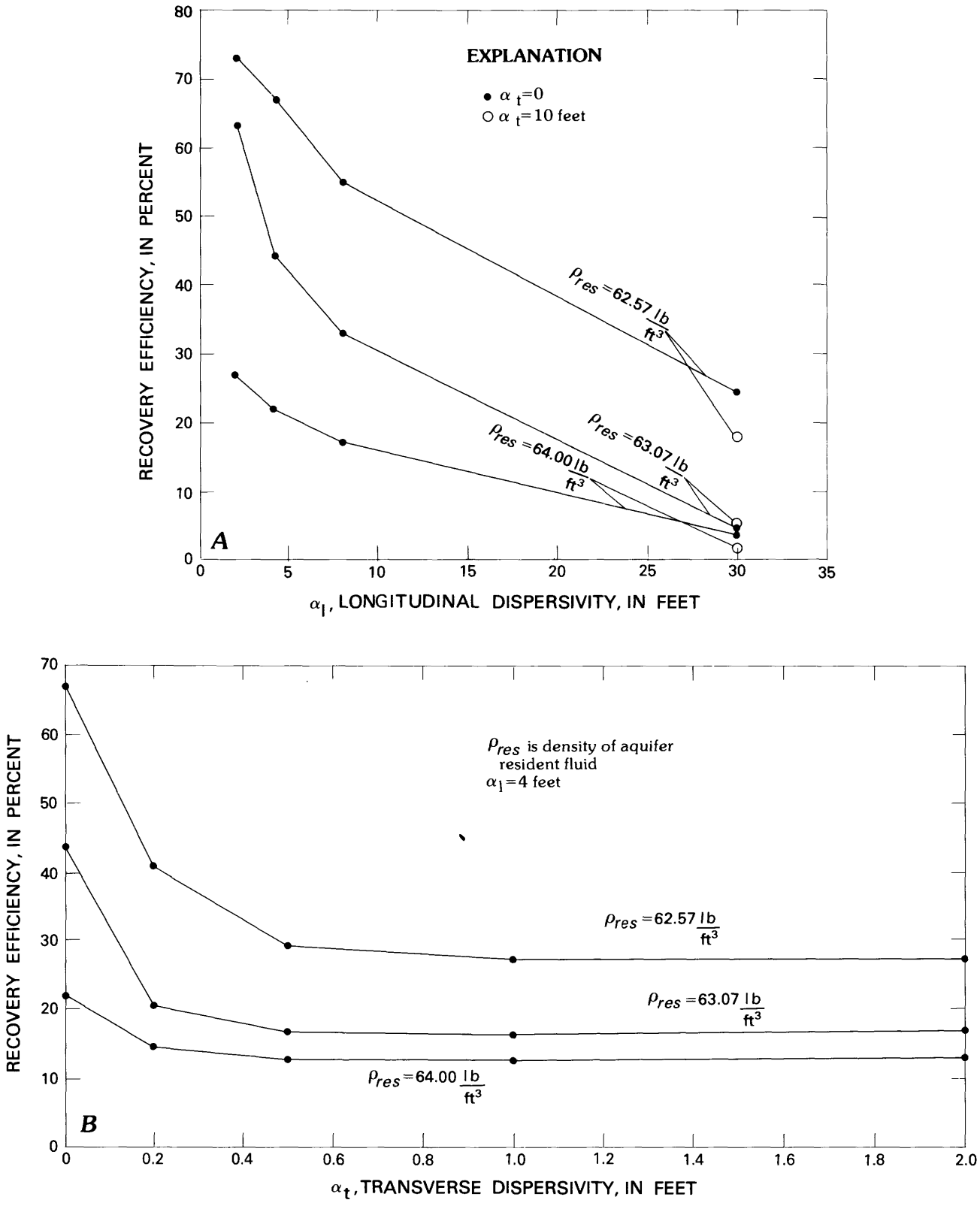

Figure 6. Relation between recovery efficiency and the degree of dispersion. *A*—variation of recovery efficiency with the degree of dispersion in the direction of flow for zero and non-zero degrees of interlayer dispersion; *B*—variation of recovery efficiency with the degree of interlayer dispersion for a constant degree of dispersion in the direction of flow. The degrees of dispersion in the direction of flow and interlayer dispersion are specified by coefficients of longitudinal dispersivity (α_l) and transverse dispersivity (α_t).

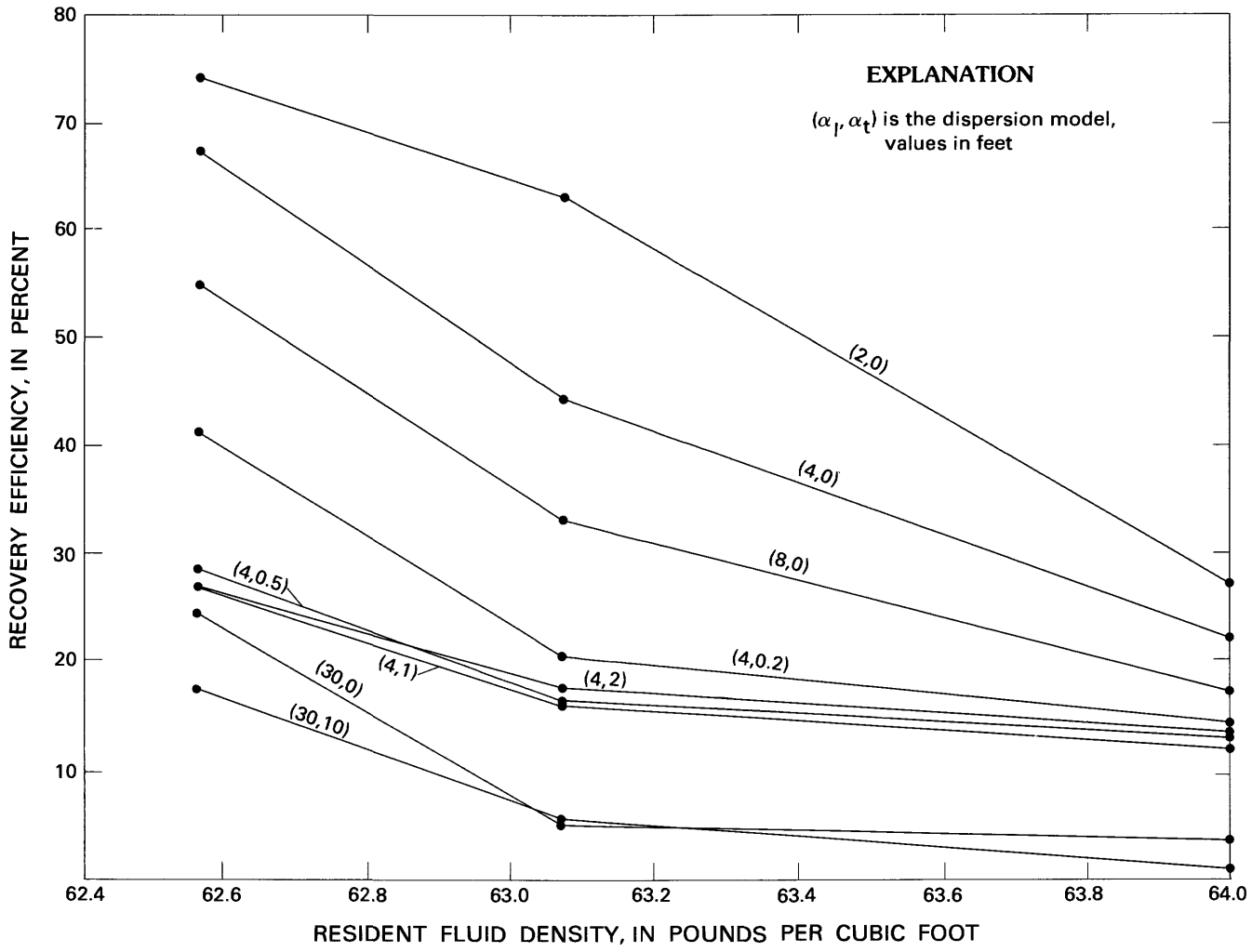

Figure 7. Relation between recovery efficiency and resident fluid density. Shown for a variety of dispersion models [choices of longitudinal dispersivity (α_l) and transverse dispersivity (α_t)].

model. The computations confirmed that as resident fluid salinity increases, a smaller part of the water within the transition zone is potable. Letting $\alpha_l = 4$ ft and $\alpha_t = 0$, the resulting transition zone was about the same width for the three densities. However, when withdrawal ceased because the salinity of withdrawn water had reached the potability limit, the radius to the 50 percent concentration (midpoint of the zone of diffusion) was about 285 ft when $\rho_{res} =$ 62.57 lb/ft^3, about 375 ft when $\rho_{res} = 63.07$ lb/ft^3, and about 450 ft when $\rho_{res} = 64.00$ lb/ft^3. The anomalous shape of the graph of the relation for the case $\alpha_l = 2$ ft, $\alpha_t = 0$ (fig. 7) may have resulted from computational instabilities which were more significant for this low dispersivity value than any other.

Aquifer Storage Capacity

The amount of injected freshwater that is recoverable may depend partly on the storage capacity (storativity) of the aquifer. This relation was studied with the cylindrical-coordinates version of the INTERA model. Storativity specification in this model is based on a conceptual model in which the storage coefficient is an algebraic combination of porosity, water density, layer thickness, and compressibility of the aquifer material and of water (Lohman, 1979). Thus, aquifer storage capacities are considered to be linearly related to thickness and porosity. Because potential injection zones in south Florida vary greatly in thickness, and to a lesser extent in porosity, a presentation of the relations of recovery efficiency to these parameters was considered to illustrate the recovery efficiency dependence on storage capacity.

The process affecting recovery in these simulations was hydrodynamic dispersion. Thus, variations in the degree of dispersive mixing resulting from differences in aquifer storage properties were the actual subject of the analysis, and results depended on the adequacy of the mathematical representation of dispersion in the IN-

TERA model. Buoyancy effects did not occur under the specified hydrogeologic conditions.

It can be assumed that recovery efficiency depends on the relative volumes of water affected by mixing within the transition zone and unaffected by mixing in the freshwater surrounded by the transition zone, although the quantitative relation may be complex. If a given volume of water is injected into a relatively thick layer, the unmixed freshwater will occupy a relatively thick cylinder of relatively small radius, and the zone of diffusion of the same vertical dimension will start at a relatively small radius from the well. This concept is illustrated by comparing figure 2*A* and figure 2*C*. Also, for a given rate of inflow, dispersion will be reduced by the lower speed of radial flow in a thicker layer so that the transition zone that develops will be narrower (fig. 2*C*). Thus, in a thicker layer, the relative volume of the transition zone will be increased by the larger vertical dimension but decreased by being narrower. This poses the question of whether the relative volume of unmixed water increases or decreases with greater layer thickness. A decrease would suggest decreased recovery efficiency.

When only dispersion in the direction of flow occurs, an analytical argument based on equation 4 answers the question. Differentiating the expression for the ratio of the volume of the transition zone to the volume of freshwater surrounded by it with respect to the zonal thickness (h), the following is obtained:

$$\frac{\partial}{\partial h}\left(\frac{V_{zf}}{V_{fw}}\right)=\frac{-A\left(\frac{V}{\pi\Theta}\right)^{-1/4}\left[A^2-\left(\frac{V}{\pi\Theta h}\right)^{1/2}\right]}{h^{3/4}\left[\left(\frac{V}{\pi\Theta h}\right)^{1/4}-2A+A^2\left(\frac{V}{\pi\Theta h}\right)^{-1/4}\right]^2}. \quad (8)$$

This has positive values when

$$\left(\frac{V}{\pi\Theta h}\right)^{1/2}=R>A^2=0.68\,, \quad (9)$$

which means that the transition zone enlarges relative to the zone of unmixed freshwater when the layer thickness increases, likely decreasing the amount of recoverable potable water. The INTERA model was applied to obtain numerical estimates of this relation in the chosen prototype aquifer for various degrees of dispersion and to study the case of interlayer dispersion.

The relation of recovery efficiency to the degree of porosity is similar and can be studied using a similar approach. For a given volume of injected water and for a given layer thickness, aquifer material of relatively high porosity will contain a freshwater cylinder of relatively small radius so that the transition zone will be relatively close to the well. On the other hand, radial outflow velocity will be reduced so that the transition zone will be narrower. A mathematical argument very similar to the preceding one shows that the volume of the transition zone enlarges relative to the volume of unmixed freshwater when porosity increases. An assumption underlying the application of the INTERA model to the study of the porosity relation was that hydrodynamic dispersion, hydraulic conductivity, and various other parameters are unrelated to porosity.

Methodology of Analysis

The five-layer radial model was used, with an initially uniform resident fluid density specification of 62.57 lb/ft^3. The three nominal dispersion models previously described were used in both the thickness and porosity analyses. In the first series of sensitivity tests, thickness values specified for the most permeable zone were 12, 24, and 48 ft. The first value was the estimated thickness of the most permeable layer at the Hialeah site. As hydraulic conductivity values were unchanged from the nominal values of the five-layer model, a large increase of injection zone transmissivity resulted from increasing the most permeable layer thickness. In the second series of tests, the most permeable layer thickness was specified to be 12 ft, and 20, 35, and 50 percent values were specified for porosity in all layers. The second value was considered the best estimate of aquifer porosity at the Hialeah site.

Results of Analysis

Increasing the layer thickness caused recovery efficiency to decrease (fig. 8) when dispersion models 1 ($\alpha_l=4$ ft, $\alpha_t=0$) and 3 ($\alpha_l=30$ ft, $\alpha_t=10$ ft) were used, and to increase when dispersion model 2 ($\alpha_l=4$ ft, $\alpha_t=1$ ft) was used.

Since flow had virtually no vertical component, dispersion model 1 was of a relatively narrow transition zone at the freshwater and saline water interface and of no dispersion between layers. When the most permeable layer was thickened, the transition zone was portrayed by the model as narrower and was located at a smaller radial distance from the well. When the layer thickness was 12 ft, the estimated radial distance between the 84 and 16 percent freshwater concentrations in the most permeable layer was about 138 ft at the end of 53 days of injection. When the layer thickness was 48 ft, this distance was about 94 ft. The radius to the 84 percent concentration decreased from 434 to 247 ft, and the volume ratio of equation 4 increased from about 74 to 91 percent, supporting the conclusion of the analytical argument that the volume of the transition zone increased relative to the volume of unmixed freshwater. As expected, this was accompanied by a 10 percent reduction in recovery efficiency.

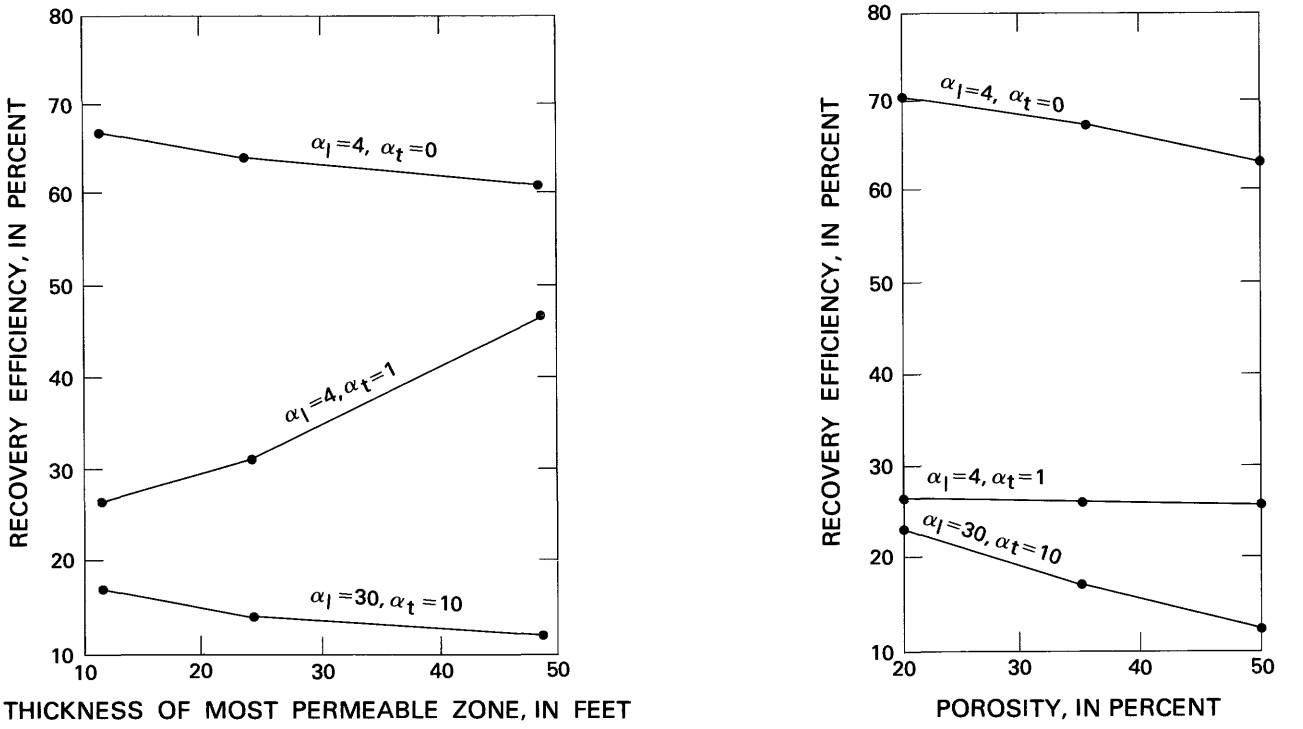

Figure 8. Relation between recovery efficiency and aquifer storativity parameters. (α_l and α_t are longitudinal and transverse dispersivity coefficients, in feet.)

Runs incorporating dispersion model 2 portrayed interlayer dispersion of freshwater into adjacent, less permeable layers and a broader transition zone in the most permeable layer. Both effects reduce the amount of recoverable potable water. Computations indicated that increasing the thickness of the most permeable layer reduced the proportion of its part of the injected freshwater that dispersed into adjacent layers and produced a narrower transition zone. Apparently, this effect was more significant than that of the relative increase of the volume of the transition zone. Figure 8 (left) shows an increase of recovery with increasing thickness. However, an inverse relation similar to dispersion model 1 appeared to apply to the case of dispersion model 3, which represented a broad transition zone and nearly complete saturation by interlayer dispersion of layers adjacent to the most permeable layer. Because of the high longitudinal dispersivity, the transition zone remained broad when the layer was thickened.

The porosity and recovery relations (fig. 8, right) had a similar interpretation for the three dispersion models.

Background Hydraulic Gradients and Length of Storage Period

Of major interest relative to the potential feasibility of freshwater injection is the effect of delaying the recovery of the injected freshwater. In south Florida, water injected during a wet season may not be needed until near the end of the subsequent dry season, or until an especially prolonged dry season several years later.

The length of storage can be significant if aquifer permeability and resident-fluid salinity are such that appreciable buoyancy stratification occurs with time, or if background hydraulic gradients move the injected freshwater downgradient from withdrawal wells. In saline aquifers in south Florida, local gradients would likely be natural rather than manmade, as supply wells would be in other aquifers where water is potable.

Hydrodynamic dispersion combines mechanical dispersion and molecular diffusion effects, which should be considered separately in relation to the effect of delayed recovery. Mechanical dispersion is an effect of flow and should not occur if the injected freshwater remains at rest within an aquifer. It would occur, however, if regional flow moves the injected freshwater a significant distance. Molecular diffusion of chloride ions from the saline resident fluid into the freshwater is usually considered to be of such small magnitude (Reeder and others, 1976) that it would have a negligible effect on a large volume of freshwater for the lengths of time relevant to freshwater storage in south Florida. Literature values for its magnitude range from 0.1 ft^2/d (Hoopes and Harleman, 1967) to 1×10^{-5} ft^2/d (INTERCOMP Resource Development and Engineering, 1976).

If there is an appreciable natural hydraulic gradient and the storage period is sufficiently long, the well would no longer be at the center of the freshwater mass during recovery. Near the end of recovery, saline water would be pumped from the upgradient direction while substantial amounts of freshwater remained in the downgradient direction. If the saline contribution were sufficient to make the withdrawn water nonpotable, the remaining freshwater would be lost. Special well arrangements can be devised to optimize recovery when an appreciable background gradient exists (Kimbler and others, 1975).

The radial dimension of the mass of injected freshwater determines the degree of displacement with respect to the well for a given hydraulic gradient and storage duration. The regional gradient in the Floridan aquifer is small at the Hialeah site, and water interstitial velocity estimates (F. W. Meyer, oral commun., 1980) range from about 0.06 ft/d (22 ft/y) to about 0.12 ft/d (44 ft/y). The higher value is suggested by recent Floridan aquifer potentiometric levels in western Broward County. Such velocities in the most permeable layer at the Hialeah site would cause injected freshwater stored for 6 months to drift about 11 to 22 ft downgradient from the injection well. If the diameter of the freshwater cylinder were hundreds of feet, the effect on recovery efficiency would be negligible. If the storage period were lengthened, however, the effect could become appreciable. The larger the volume injected and the greater the radial dimension, the longer could be the storage period before an appreciable displacement would take place. If aquifer thickness were so large that a large volume of injectant occupied a cylinder of small radius about the well, a short storage period might be sufficient to cause appreciable movement. These conclusions were partly illustrated with applications of the INTERA model.

Methodology of Analysis

The first test was to verify the assumption that molecular diffusion would not cause any significant reduction in recovery efficiency during a 6-month storage period when no regional flow took place, and when hydrologic conditions did not favor any appreciable level of buoyancy stratification., The six-layer radial model with the vertically heterogeneous Hialeah chloride distribution was used. Maximum density was specified to be 62.50 lb/ft^3, and dispersion model 1 was used. The 53-day injection phase was followed by a storage period of 187 days, simulated by specifying a zero inflow rate for the well. The value chosen for the level of molecular diffusion was 0.001 ft^2/d.

Remaining tests were of the effects on recovery efficiency of regional flow in the Floridan aquifer during storage periods of various durations. Radial symmetry was no longer a valid assumption. Thus, the INTERA model was applied to represent lateral flow confined above and below in the 12-foot most permeable layer discretized into a rectangular 27×27 grid. Adjacent layers were not represented. The density of the resident fluid was specified to be 62.57 lb/ft^3. The longitudinal dispersivity coefficient of 4 ft represented a relatively sharp transition zone, a useful approach for defining small regional drift effects. Regional Darcian flow rates of 0.022 ft/d and 0.044 ft/d were represented as occurring along the X-axis of the grid, and constant boundary pressure values were entered to maintain simulated flow at these rates.

Analyses incorporating regional flow and showing the dependence of recovery efficiency on aquifer storativity and on the volume of injection were not made.

Results of Analysis

Results of the test for molecular diffusion effects showed that, at the end of the storage period, the chloride concentration distribution was virtually the same as at the end of the injection period. The lack of any consistency to the slight variation of some concentrations indicated that this variation was due merely to a low level of numerical oscillation.

Areal simulations incorporating estimates of south Florida's regional flow portrayed a slight asymmetry along the X-axis of the concentration distribution at the end of 53 days of injection. When no regional flow was simulated, recovery efficiency was about 60.9 percent. When regional flow (22 ft/y) was simulated and withdrawal began immediately after injection, the computed recovery efficiency was virtually unchanged. When a 6-month storage period preceded withdrawal, a recovery efficiency of about 60.5 percent was computed. When the regional flow was 44 ft/y, recovery efficiency was computed to be 59.9 percent after a 6-month storage period. The slight drift of the freshwater mass (44 ft/y) during the 6-month storage period is illustrated in figure 9*A*, and the residual unrecoverable potable water at the end of withdrawal is shown in figure 9*B*. The storage period simulation introduced significant row-wise oscillations.

When regional flow of 44 ft/y and a storage period of 5 years were simulated, recovery efficiency was computed to be 21.8 percent. The substantial drift of the freshwater mass during the storage period is shown in figure 9*A*. The simulation portrayed significant hydrodynamic dispersion after the injectant had moved some distance; thus, the 250 mg/L chloride line shows some compression along the axis of movement. The residual unrecoverable potable water at the end of recovery is shown in figure 9*B*.

Simulations showed that the effect of regional flow in the most permeable layer of the injection zone at the

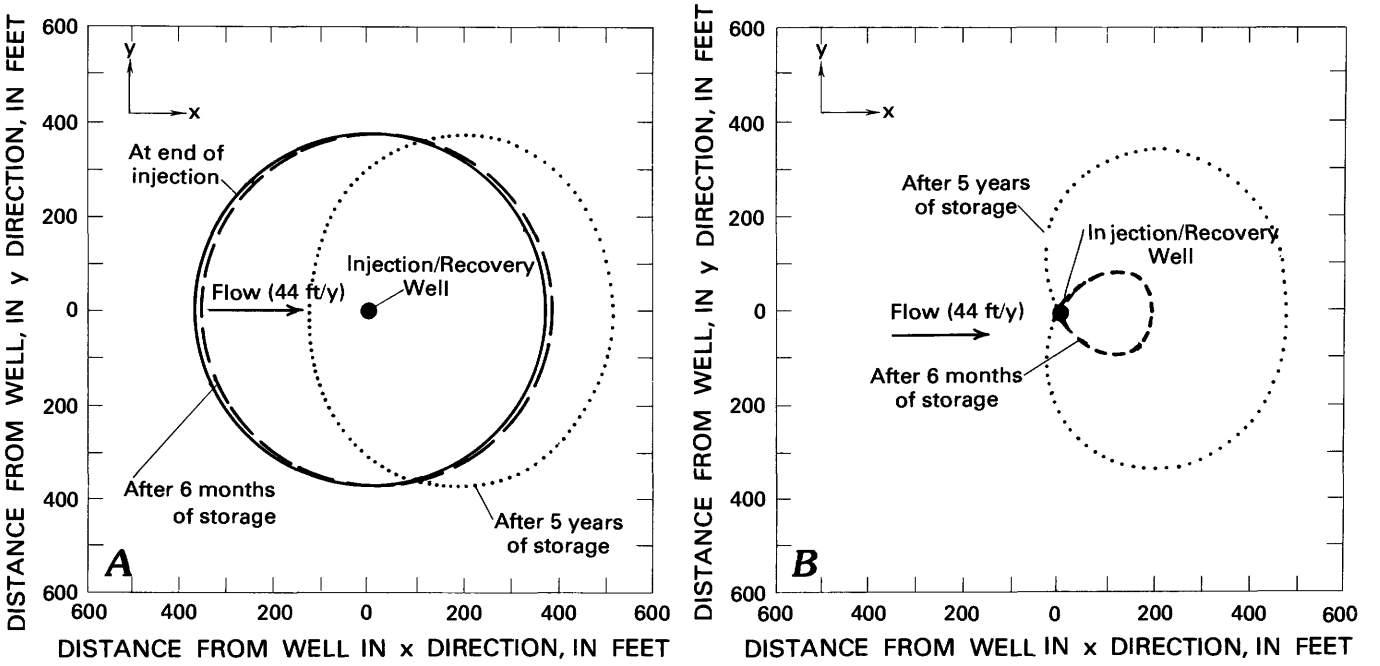

Figure 9. Effect of regional flow on the position and recoverability of potable water. *A* and *B* are overhead views. *A*—potable water (chloride concentration less than 250 milligrams per liter) is contained in the volumes within the circular and elliptical outlines corresponding to the indicated times. *B*—contained within the outlined volumes is unrecoverable potable water remaining in storage when withdrawn water exceeded 250 milligrams per liter of chloride. X and Y are axes of Cartesian coordinates. Constant and uniform regional flow (44 feet per year) is represented as occurring in the positive X direction.

Hialeah site was negligible when recovery began immediately after 53 days of injection and also when a 6-month storage period intervened, even if the regional gradient was 44 ft/y. When simulated storage was for 5 years, recovery efficiency was reduced to about one-third of the original value. Results indicate that, although it can be feasible to store freshwater for certain periods in south Florida without substantial loss of recoverable water, site-specific analyses would be required to determine storage period limitations at particular locations. Although not illustrated by model analyses, the volumes of freshwater to be injected and the thickness of the principal receiving zone are important factors in this determination.

DEPENDENCE OF FRESHWATER RECOVERY ON DESIGN AND MANAGEMENT PARAMETERS

Rates of Injection and Recovery

Injection or withdrawal at higher rates has the advantage of requiring less time for a given volume and the disadvantage of requiring higher pump pressures. A range of feasible rates may be established by the hydrogeologic setting and design features of a proposed system. Thus, it is of interest to know if the rate of injection or withdrawal affects the amount of potable water that can be recovered.

The degree of hydrodynamic dispersion, which limits recovery efficiency, is represented in the INTERA model as linearly proportional to the velocity of flow, which increases with the rate of injection or withdrawal. However, for a fixed volume, the duration of the injection or withdrawal period during which flow and dispersion occur decreases when the rate increases. Equations 3 and 6 suggest that, when only dispersion in the direction of flow occurs and when the degree of molecular diffusion is negligible compared with the degree of dispersion, the width of the transition zone should be related to volume injected rather than to the rate of injection. Equivalently, the width of the transition zone would be related to the extent of outward movement of freshwater from the well. The question posed for model sensitivity testing was whether the rate of injection or withdrawal of a fixed volume of freshwater would affect the degree of dispersion, and, hence, recovery efficiency.

Methodology of Analysis

The five-layer radial model with uniform initial resident fluid density of 62.57 lb/ft^3 was used. Computations were made for the three standard dispersion

models, and also for two other models specifying no interlayer dispersion ($\alpha_l = 2$ ft, $\alpha_t = 0$, and $\alpha_l = 30$ ft, $\alpha_t = 0$), for the purpose of revealing any effect on the rate relation of the type and degree of dispersion. To test the effect of a small degree of interlayer dispersion, further test runs with the same range of rates and durations were made for two additional dispersion models: $\alpha_l = 4$ ft, $\alpha_t = 0.01$ ft, and $\alpha_l = 4$ ft, $\alpha_t = 0.1$ ft.

The variables of the first series of tests were rate and duration of injection. These were adjusted so that the total volume injected was constant at 5,600,032 ft^3 and ranged from a 10-day injection at 560,003 ft^3/d to a 200-day injection at 28,002 ft^3/d. Withdrawal rate in all these runs was 62,047 ft^3/d. The variable of the second series of tests was withdrawal rate, varying from 15,000 ft^3/d to 250,000 ft^3/d. This followed injection at 105,661 ft^3/d for 53 days, so that the total stored volume was 5,600,032 ft^3.

Results of Analysis

Generally, the analyses indicated that no relation existed between the rate at which a given volume of water was injected or withdrawn and the amount of potable water that could be recovered. The small, inconsistent variations that occurred were believed to be within the solution accuracy of the model. This held for any levels of hydrodynamic dispersion in the direction of flow or between layers which were specified by the longitudinal and transverse dispersivity coefficients. The width and placement of transition zones appeared to be unrelated to the specified rates. The INTERA computations seemed to support the implication of equation 3 that the development of a transition zone is related to the extent of interface movement rather than to the rate at which the movement occurred. Results of these analyses depend on the adequacy of the INTERA model representation of dispersion.

Well Not Open to Full Thickness of Injection Zone

In all previous analyses, it was assumed that the well used for injection and withdrawal was open to the entire permeable thickness, as well as to sections of overlying and underlying relatively impermeable confining layers, as was the case at the Hialeah site. However, operational wells may be open only to part of an aquifer. Thus, it is of interest to compare the recovery efficiency of a well open only to part of the thickness of a permeable layer (partially penetrating) with recovery efficiency of a well open to the full thickness.

Near a well open only to part of a permeable zone, vertical hydraulic gradients between the open interval and adjacent permeable layers may cause appreciable vertical flow of injected freshwater into the adjacent layers during injection and from them during withdrawal. The cylindrical-coordinates version of the INTERA model was used to illustrate the pattern of flow from a well in this case and to calculate recovery efficiency relative to the case of a well open to the entire permeable zone.

Methodology of Analysis

The six-layer radial model was applied, with an initially vertically uniform resident fluid density of 62.50 lb/ft^3. Tests were made for each of the three standard dispersion models. The well index and other input to the INTERA model were modified to represent injection into layers 4, 5, and 6 only. Thus, the well was open to the lower 4 ft of the most permeable layer, to the underlying, relatively less permeable 23-foot layer, and to the next underlying, virtually impermeable layer. The well was not open to the upper 8 ft of the most permeable layer (layer 3) or to overlying, less permeable layers. Total injection and withdrawal rates were the same first Hialeah test values as for control runs of full aquifer penetration. The low resident fluid density and the Hialeah site hydraulic conductivity values ruled out the occurrence of any appreciable buoyancy effects during the simulation time of the tests, so that vertical flow was entirely due to hydraulic gradients from injection and withdrawal.

Results of Analysis

Recovery efficiencies are shown below, for the three dispersivity models, comparing injection into layers 4 to 6 with control simulations of injection into all six layers.

Dispersivity model	*Recovery efficiency (percent) Well open to:*	
	Layers 4–6	*Layers 1–6*
1	67.5	66.0
2	26.2	27.4
3	17.4	17.7

Considering the major alteration of the flow field, the recovery amounts are remarkably similar. In fact, differences are small enough to be considered within solution accuracy. The computed distributions of freshwater and saline water in the six-layer interval after 53 days of injection were very similar. Results suggest that recovery efficiency in stratified aquifers in south Florida might not be affected if the well is open to only part of a permeable layer.

Simulations of injection into layers 4 to 6 portrayed appreciable vertical hydraulic gradients and vertical flow of freshwater into adjacent permeable layers 3 and 2 near the well (fig. 10*B*). This was unlike the control simulation (well open to all layers), in which pressure adjusted to a

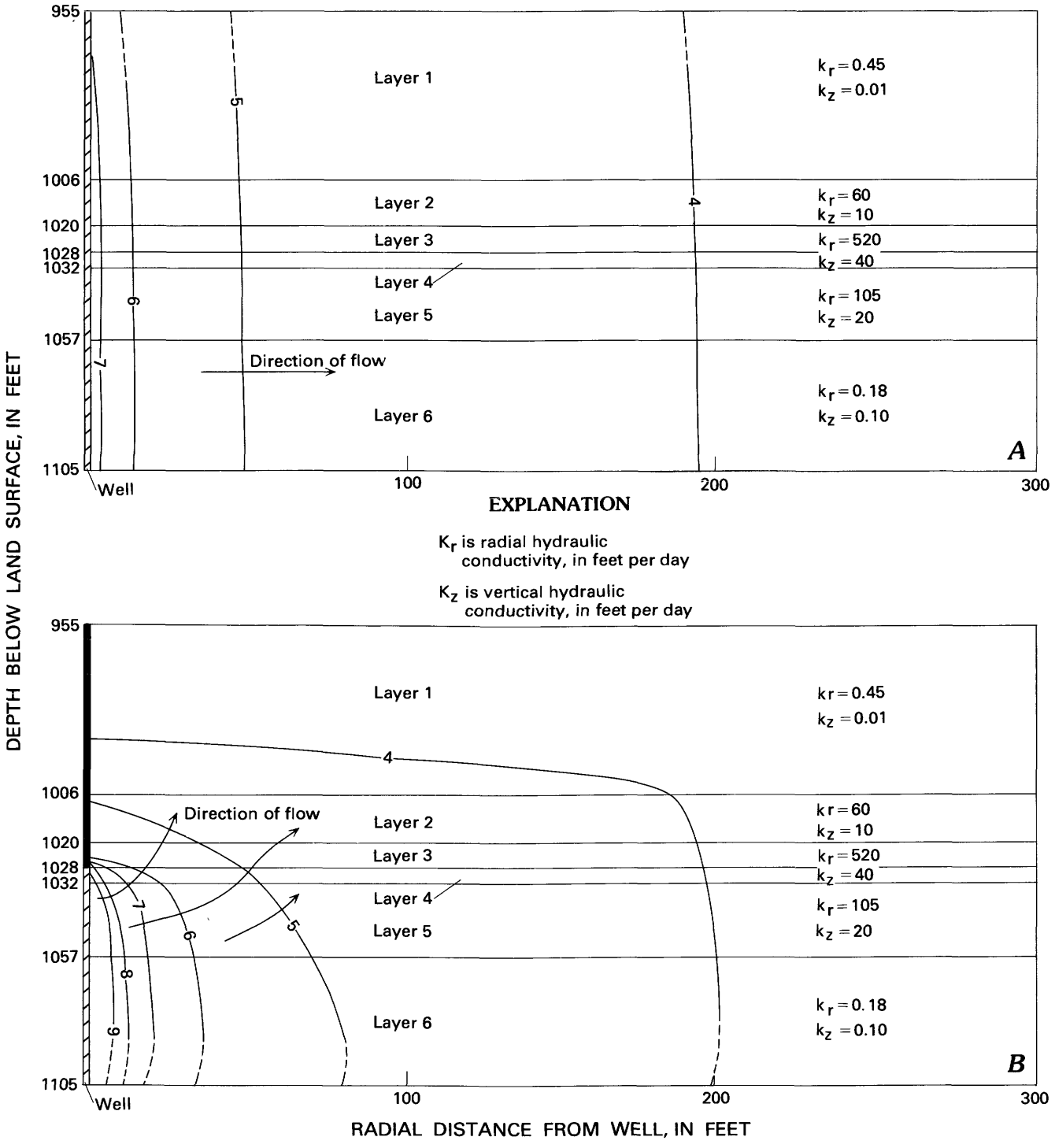

Figure 10. Pressure increases during injection when: *A*—well is open to all permeable layers and *B*—well is open to only part of permeable zone. Values are in pounds per square inch. Total injection rate is the same in both cases. Pressure values have been adjusted to a common datum.

common datum was nearly uniform vertically and vertical flow was negligible (fig. 10*A*). Flow into layer 1 was negligible, owing to the very small vertical permeability of that layer. At radii greater than 300 ft (not shown), common-datum pressure was nearly uniform vertically at about the same magnitude as in the control simulation, showing that flow had virtually no vertical component at that distance from the well.

Volume of Water Injected

Relative volumes of unmixed injected freshwater and injected freshwater mixed with resident water within the transition zone surrounding the unmixed freshwater (fig. 2A) partly determine the amount of potable water that can be recovered, as previously shown. Thus, if the relative volume of the transition zone does not increase in direct proportion to an increase of total volume injected, the relative proportions of unmixed and mixed water will change, causing recovery efficiency to change also.

To determine the nature of this relation when no interlayer dispersion occurs, the expression (equation 4) for the ratio of the volume of the transition zone to the volume of freshwater encircled by it can be differentiated with respect to the injected volume (V):

$$\frac{d}{dV}\left(\frac{V_{zf}}{V_{fw}}\right)=\frac{-AV^{-1}\left(\frac{V}{\pi\Theta h}\right)^{-1/4}\left[\left(\frac{V}{\pi\Theta h}\right)^{1/2}-A^2\right]}{\left[\left(\frac{V}{\pi\Theta h}\right)^{1/4}-2A+A^2\left(\frac{V}{\pi\Theta h}\right)^{-1/4}\right]^2}. \quad (10)$$

This has negative values when $(V/\pi\Theta h)^{1/2}=R>A^2=0.68\alpha_l$, indicating that the relative volume of the transition zone decreases with larger injected volumes. Thus, the proportion of unmixed water should increase, and the recoverable amount of potable water should also increase. This was verified in a series of tests with the cylindrical-coordinates version of the INTERA model, and the case of interlayer dispersion was also studied.

Methodology of Analysis

The five-layer radial model was used, with a vertically uniform resident fluid density of 62.57 lb/ft^3. Tests were performed using the three standard dispersion models and an additional dispersion model in which $\alpha_l=4$ ft, and a low level of interlayer dispersion was specified ($\alpha_t=0.1$ ft). The total volume injected was varied by specifying 53-day injection rates (Q_i) ranging from 10,000 ft^3/d to 250,000 ft^3/d. For a given volume, the selected injection and withdrawal rates are unrelated to recovery efficiency, as shown in a previous analysis, so that this was an appropriate way to illustrate the relation between volume and recovery efficiency. As in other analyses, results are understood to depend on the adequacy of the mathematical representation of dispersion in the INTERA model.

Results of Analysis

Disparate trends for the various dispersion models are evident (fig. 11). All the curves show that for sufficiently small injected volumes, recovery efficiency increases with increasing injected volume. When dispersion model 1 was assumed, the increase of recovery efficiency with volume continued through the entire range of volumes tested, though the rate of increase declined with increasing volume. This supported the conclusion of the analytical argument that, if no interlayer dispersion occurred, the deleterious effect of dispersive mixing in the direction of flow lessened with increasing volume.

When a small degree of interlayer dispersion was assumed to occur ($\alpha_t=0.1$ ft), recovery efficiency increased in the low-volume range but decreased slowly in a higher range (fig. 11). When a higher degree of interlayer dispersion was specified (dispersion model 2), the recovery efficiency change was virtually negligible after an increase in the low-volume range. When dispersion model 3 was used, dispersive mixing affected nearly all injected water in the low-volume range and greatly limited the slowly increasing recovery efficiency for larger injection volumes.

A study of the nonuniform vertical distribution of salinity when withdrawn water became saline (see section on hydrodynamic dispersion) showed different degrees of the influence of interlayer dispersion. When $\alpha_l=4$ ft and $\alpha_t=0.1$ ft, the pattern was like the case of no interlayer dispersion for small volumes and like the case of appreciable interlayer dispersion for large volumes. When $\alpha_t=1$ ft, the pattern showed the influence of interlayer dispersion for small and large volumes.

Successive Cycles of Injection and Recovery

Cyclic injection in south Florida may be based on the annual wet and dry season cycle, with yearly repetitions of injection during the wet season and withdrawal during the dry season. Thus, of major interest is whether recovery efficiency changes with successive cycles, in each of which the withdrawal phase ceases when withdrawn water becomes too saline to be potable.

Assuming no background hydraulic gradients, buoyancy, or permeability changes, the process affecting recovery efficiency is hydrodynamic dispersion. Dispersive mixing processes, continuing as residual freshwater returns to the well during withdrawal, gradually increase the chloride concentration of the withdrawn water. If withdrawal is stopped when withdrawn water exceeds potability (250 mg/L of chloride), the chloride distribution in the aquifer at that time becomes the initial distribution for the next injection phase. This saline mix of injected freshwater and native water about the well mixes with additional freshwater during the next injection to form a new transition zone. Thus, with each successive injection, the transition zone becomes progressively broader and more diffuse from the accretion of residual freshwater from previous injections, and more

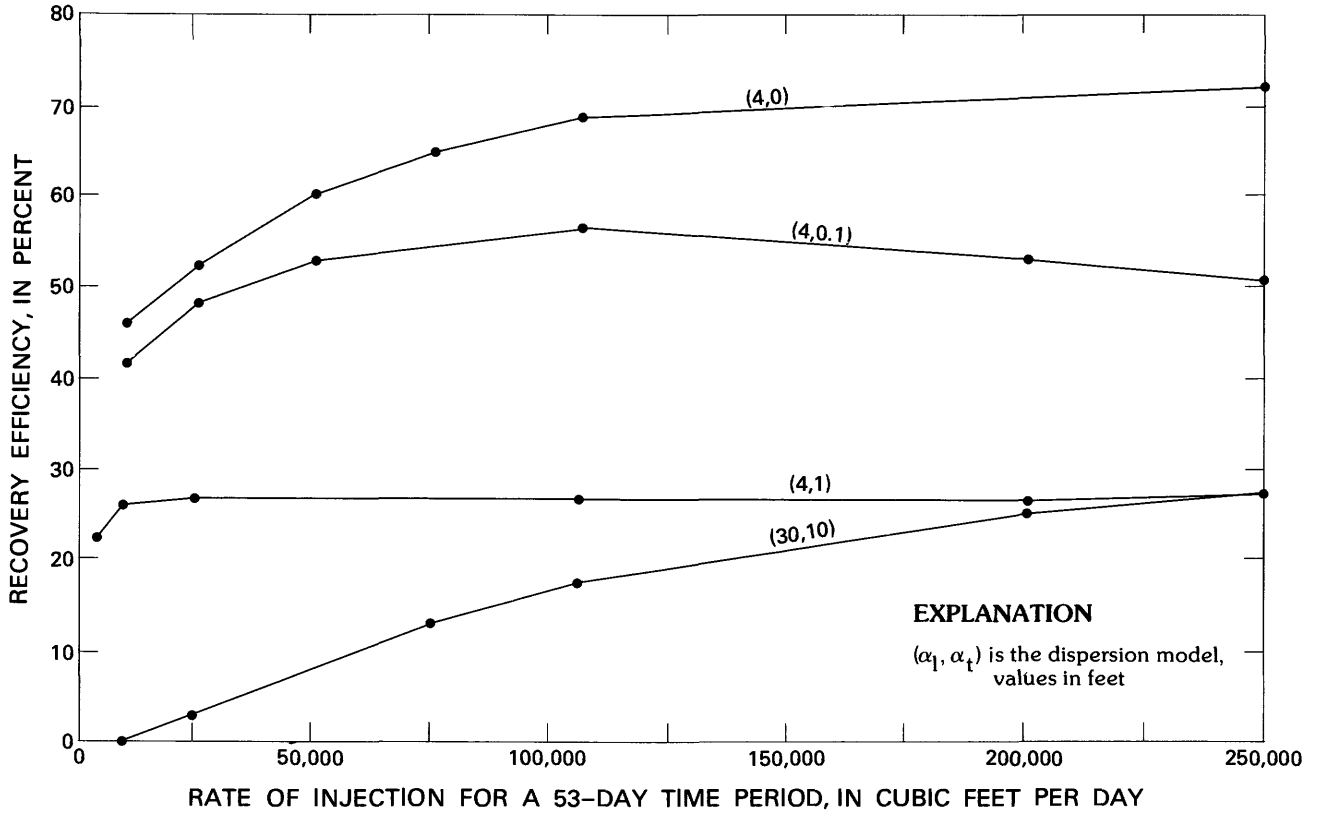

Figure 11. Relation between recovery efficiency and volume of freshwater injected. Shown for four dispersion models [choices of longitudinal and transverse dispersivity coefficients (α_l and α_t)].

of the mixed water is potable. A progressive increase in recovery efficiency would be expected. This concept was tested with the cylindrical-coordinates version of the INTERA model.

Methodology of Analysis

The five-layer radial model with a uniform initial resident fluid density of 62.57 lb/ft^3 was used. Tests were made for each of the three standard dispersion models, and also for four additional models to better demonstrate the dependence on dispersion. The dispersivity parameters for the four additional models were as follows: $\alpha_l = 2$ ft, $\alpha_t = 0$; $\alpha_l = 8$ ft, $\alpha_t = 0$; $\alpha_l = 20$ ft, $\alpha_t = 0$; and $\alpha_l = 30$ ft, $\alpha_t = 0$.

In the first series of tests, 12 successive 53-day regimes of injection at the rate of 105,661 ft^3/d were simulated. Each was followed by a recovery phase with a withdrawal rate of 62,047 ft^3/d, which lasted until withdrawn water reached a chloride concentration of 250 mg/L. All dispersion models described above were incorporated into this series of tests.

In the second series of tests, a hypothetical wet and dry season schedule was simulated. Freshwater was injected from June through October (153 days) and was withdrawn beginning February 1 at a rate of 265,000 ft^3/d (about 1,375 gal/min or 2×10^6 gal/d). Withdrawal ceased when the withdrawn water reached a chloride concentration of 250 mg/L or after 120 days (February through May), whichever occurred first. The objective was to determine the concentration of the withdrawn water at the end of 120 days, if still potable, and to show how this 120-day concentration decreased with successive annual cycles. Only the three standard dispersion models were used in this second series of tests.

Results of Analysis

Results of the first series of tests are shown in figure 12*A*. For each dispersion model, recovery efficiency improved with each repetition of the cycle, though the

Figure 12. Improvement of recovery efficiency with successive injection and recovery cycles. *A*—rate of improvement for a variety of dispersion models (choices of dispersivity coefficients α_l and α_t); *B*—decrease of the chloride concentration of withdrawn water after 120 days of recovery. If the chloride concentration exceeds 250 milligrams per liter earlier than 120 days, withdrawal is ended at that time and 250 milligrams per liter is the value plotted.

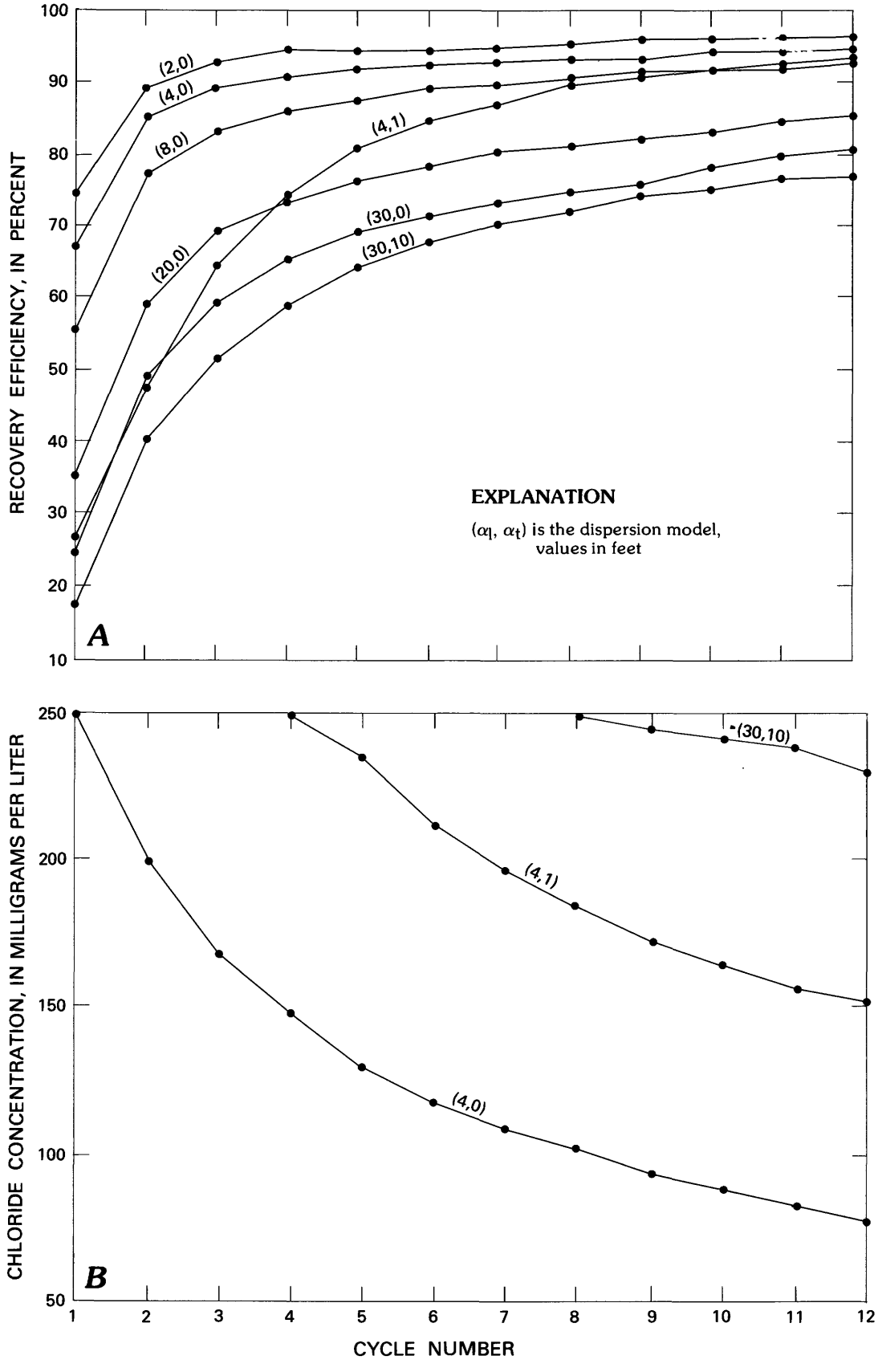
RECOVERY EFFICIENCY, IN PERCENT
100
90
80
70
60
50
40
30
20
10
(2,0)
(4,0)
(8,0)
(20,0)
(4,1)
(30,0)
(30,10)
EXPLANATION
(α_l, α_t) is the dispersion model, values in feet
A
CHLORIDE CONCENTRATION, IN MILLIGRAMS PER LITER
250
200
150
100
50
(30,10)
(4,1)
(4,0)
B
1
2
3
4
5
6
7
8
9
10
11
12
CYCLE NUMBER

rate of improvement decreased with successive cycles. For low degrees of dispersion in the direction of flow ($\alpha_l = 4$ ft) and no interlayer dispersion, most improvement occurred in the first four cycles; for higher degrees of dispersion ($\alpha_l = 30$ ft), it was more gradual. After 12 cycles, recovery efficiency was computed to be 96.8 percent for $\alpha_l = 2$ ft, 93 percent for $\alpha_l = 8$ ft, and 80.9 percent for $\alpha_l = 30$ ft. Recovery efficiencies at the end of the first cycle had been 74, 56, and 24 percent. It is unknown what the ultimate limit of recovery efficiency would be after an infinite number of identical cycles.

At the end of each successive injection cycle, the transition zone became gradually more diffuse, with the 50 percent concentration radius progressively farther away from the well (illustrated for two of the dispersion models in fig. 13). The greater distance to the transition zone after four cycles when $\alpha_l = 30$ ft does not mean higher recovery efficiency, because higher dispersion will cause saline water to reach the well earlier during withdrawal than if $\alpha_l = 4$ ft.

These results are of considerable significance for cyclic injection feasibility. They indicate that even when a high degree of dispersive mixing reduces recovery efficiency to 20 or 30 percent in the initial cycle, recovery efficiency may improve to nearly 80 percent after several additional cycles, provided that no nonpotable water is withdrawn.

When $\alpha_l = 4$ ft and some degree of interlayer dispersion was simulated ($\alpha_t = 1$ ft), recovery efficiency in the first cycle was 41 percent less than when $\alpha_t = 0$, but improvement was more rapid. The difference in recovery efficiencies after 12 cycles was only about 1 percent. In early cycles, the simulation portrayed considerable freshwater loss to adjacent, less permeable layers by interlayer dispersion. In later cycles, these layers were shown as containing freshwater at the beginning of the injection phase.

Results of the second series of tests (fig. 12*B*) showed the decrease in the final chloride concentration after 120 days of withdrawal in successive cycles. When $\alpha_l = 4$ ft and $\alpha_t = 0$, the first recovery ended after 109 days when the withdrawn water reached a chloride level of 250 mg/L. In successive recoveries, however, withdrawal continued for the maximum allowable time of 120 days. The final chloride concentration decreased to 78 mg/L after 12 cycles, only slightly greater than that of the injected water (65 mg/L). When some interlayer dispersion was simulated (dispersion models 2 and 3), the final chloride concentration decreased more slowly, and the 12-cycle value was higher.

Well-bore Plugging

Recovery efficiency can be appreciably reduced if the spatial distribution of permeability changes from one phase of cyclic injection to another. For example, if preferred flow directions within the lateral plane of flow (anisotropic lateral permeability) during injection changed in some way during withdrawal, the pattern of flow in the lateral plane would be different during withdrawal than during injection. The radial distribution of inflow velocity within the plane of flow would not be the same as that of outflow velocity. This means that saline water in the transition zone, returning toward the well, would arrive from some directions earlier than from others, making the withdrawn water saline even while potable water remained in storage. Recovery efficiency would be reduced.

Changes in permeability might also occur along the vertical axis. In this case, aquifer layers could be considered to have a different vertical distribution of lateral permeability during the injection phase than during the withdrawal phase, and thus to have different proportions of total flow. However, only changes in lateral permeability were considered in this analysis.

Changes in the lateral distribution of permeability might occur as the result of well-bore plugging. An initial permeability anistropy may exist, owing to the orientation of solution features or to the uneven lateral distribution of the larger aquifer material pore spaces. Plugging by particulate matter in the injectant or by a precipitate from a chemical reaction might reduce permeability to a greater degree in the direction of smaller pore spaces than in the preferred flow direction. In this way, natural anisotropy would be enhanced by the injection process. However, when withdrawal begins, the plugging material might be flushed out, partly restoring the original anisotropic permeability distribution.

Like interlayer dispersion, directionally biased plugging is a hypothesis not directly confirmed by any field data, but it could explain apparent inconsistencies in pressure data, chemical data, and geophysical logging data acquired during the Hialeah injection tests (F. W. Meyer, oral commun., 1980). Well-bore plugging during injection is known to have occurred, and anisotropic lateral permeability was suspected. As south Florida aquifers are of secondary porosity limestone, lateral permeabilty anisotropy might characterize any aquifer selected for the underground storage of freshwater.

The single-layer Cartesian coordinates version of the INTERA model was used to simulate this concept and to assess the effect on recovery efficiency. An assumption of the model is that dispersivity remains isotropic even when permeability is not. Nevertheless, the degree of dispersion was lower in the less preferred flow directions as a result of the lower flow velocities.

Methodology of Analysis

The analyses consisted of assessing the effect, in terms of recovery efficiency, of directionally biased plug-

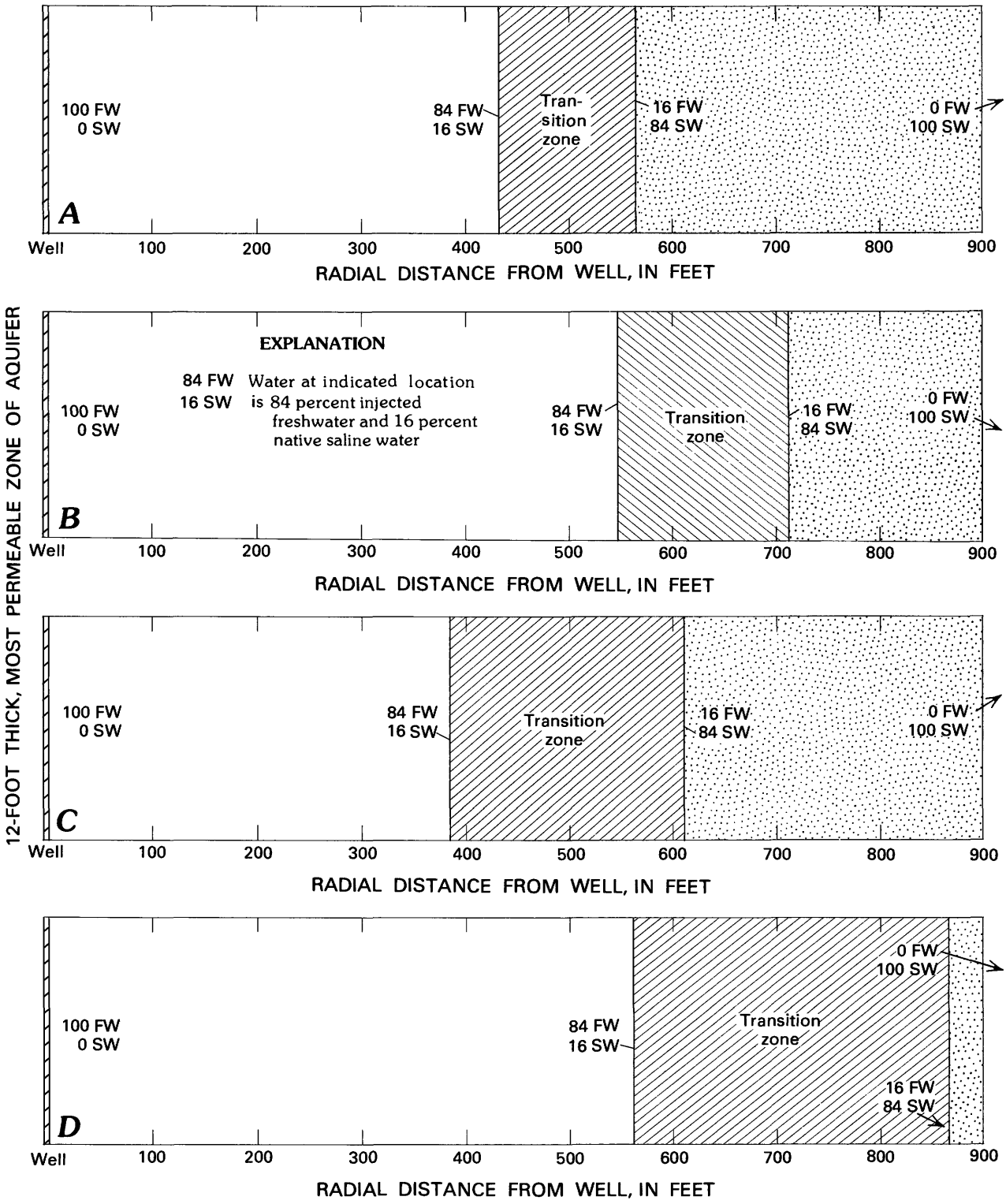

Figure 13. Displacement and broadening of the transition zone with successive injection and recovery cycles. *A*, *B*—transition zone at the end of the first and fourth identical injection cycles when the degree of dispersion in the direction of flow is specified by a longitudinal dispersivity coefficient (α_l) of 4 feet. *C*, *D*—transition zone at the end of the first and fourth injection cycles when $\alpha_l = 30$ feet. In all figures, interlayer dispersion is assumed not to occur by the specification of a transverse dispersivity coefficient value of zero.

ging by comparing the case in which plugging changes permeability with a control simulation representing the case in which the lateral distribution of permeability remains constant, as is usually assumed. A straightforward way of doing this was to assume isotropic permeability in the control simulation. Thus, in the sensitivity test, the effect of plugging was fully represented by the simulated anisotropy during injection, and permeability was considered isotropic during withdrawal. This was considered a representative test even though the isotropic model may not match conditions in a real aquifer even during withdrawal. This representation was also a generalization in other ways. Plugging does not actually occur beyond the limit of injected water, but model limitations made it convenient to assume that permeability in the less preferred flow direction decreased uniformly throughout the grid. Also, plugging actually does not instantaneously decrease permeability to a level thereafter constant, but decreases it gradually over a period of hours or days.

The decrease of permeability during injection was considered to occur along one axis of planar coordinates. Directional plugging, if it actually occurs, probably would not exhibit such symmetry, but this assumption was convenient for analysis and did not affect the generality of the result. Anisotropy during the injection phase could, thus, be represented by varying the ratio of the two principal components of the two-dimensional hydraulic conductivity tensor (k_x and k_y). The components were assumed to be in a ratio of 0.115 (k_y smaller) during injection and to be equal during withdrawal. The value of 0.115 was selected because it made the rate of outflow from the well along the coordinate axis of lower permeability consistent with the arrival time of freshwater at the observation well in the first Hialeah injection test. This was the only known basis for an estimate of plugging-induced anisotropy.

The 12-foot most permeable layer of the hypothetical aquifer was discretized as a single layer into a symmetric 27×27 grid in which the well was centered in a block 20 ft on each side. The density of the resident fluid was specified to be 62.57 lb/ft^3. Various dispersion models used in the analysis were:

Dispersivity (feet)	
Longitudinal	*Transverse*
2	0
4	0
4	1
4	4
30	0
30	10

Longitudinal and transverse dispersion in this two-dimensional areal simulation were in the plane of flow, in and perpendicular to the direction of flow. No interlayer dispersion was represented. Some row and column oscillation occurred during the simulations with INTERA, though not to a severe enough degree to prevent an interpretation of results.

Results of Analysis

The sensitivity tests portrayed a significant decrease in recovery efficiency when well-bore plugging made permeability anisotropic during the injection phase. The INTERA model computed decreases ranging from 50 to 60 percent for the various dispersion models. Recovery efficiencies computed for the various dispersion models are shown in the following table:

Dispersivity (feet)		*Recovery efficiency (percent)*	
Longitudinal (α_l)	*Transverse* (α_t)	*Isotropic* ($k_y/k_x = 1$)	*Anisotropic* ($k_y/k_x = 0.115$)
2	0	66.5	26.7
4	0	60.9	25.6
4	1	—	25.8
4	4	60.1	—
30	0	35.0	17.3
30	10	—	17.6

A comparison of recovery efficiencies when the value of lateral transverse dispersivity was varied showed little or no sensitivity to this parameter. This seemed to be characteristic of all of the single-layer radial flow simulations.

The elliptically shaped pressure field resulting when the coordinate permeability ratio was 0.115 was shown in figure 5*A*, and figure 5*B* shows the freshwater distribution at the end of injection. Figure 14 shows the shape of the freshwater mass at various simulation times during recovery after permeability isotropy is restored by clearing of the well-bore at the beginning of withdrawal. Figure 14*A* shows that improvement of flow along the Y-axis led to rapid migration of saline water toward the well along that axis. In figure 14*B*, saline water had reached the well, contaminating the withdrawn water, even though substantial amounts of potable water remained in storage along the X-axis. Figure 14*C* shows that 24 days after contamination of withdrawn water, substantial amounts of potable water remained in storage isolated from the well, which was surrounded by saline water. These freshwater slugs were depleted gradually as withdrawal continued. Computations showed that after 122 days of withdrawal, smaller but still appreciable slugs of potable water remained. By this time, the amount of potable and saline water withdrawn had far exceeded the volume injected.

Multiple-Well Configurations

An implementation of the cyclic injection concept on a major scale could require more than one well if the volumes to be injected, and the required inflow rates, exceed the capacity of a single well. The distribution of inflow might also be considered safer in that it reduces well-bore pressure and pressure in the surrounding aquifer. This reduces the chance of fracturing the injection zone or confining formations and reduces the chance of damaging the well itself.

The recovery efficiency of a group of wells depends on the extent of their interaction. Even if the wells are so spaced that the freshwater bodies about each do not merge, the hydraulic gradients from nearby wells will modify the rate and direction of freshwater movement during inflow and outflow. If the freshwater bodies make contact, they may form a common transition zone with adjoining saline water, or the intervening saline water may be displaced by freshwater flow so that two or more wells are contained within a single mass of freshwater. If wells influence each other in such a way that appreciable amounts of freshwater remain in the aquifer when water withdrawn from the wells has become too saline for potability, recovery efficiency is reduced. Whether or not this occurs may depend on the geometric arrangement of the wells, or on the schedule of injection and withdrawal at each one. Model tests were designed to study these effects.

Recovery efficiency from a particular arrangement of wells would likely be altered if regional flow causes movement of the injected freshwater (Kimbler and others, 1975). In this analysis, it is assumed that there are no background hydraulic gradients. Another assumption is that flow is uniform in an isotropic aquifer. Results of the analysis might not apply to aquifers in which actual conditions depart from these assumptions.

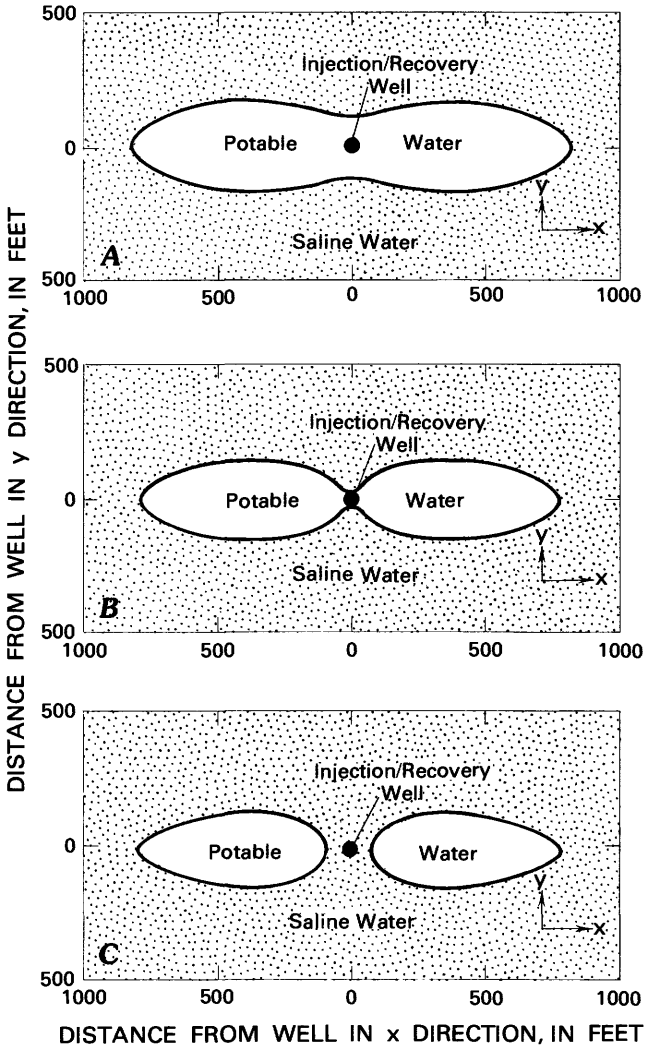

Figure 14. Distribution of potable water at successive stages of withdrawal, showing the effect of directionally biased well-bore plugging during injection. $k_y/k_x = 0.115$, where k_x and k_y are permeability components in the X and Y coordinate directions. Remaining potable water is shown: *A*—after 15 days of withdrawal, when the computed concentration of recovered water was 100 milligrams per liter; *B*—after 23 days of withdrawal, when the computed chloride concentration of recovered water had almost reached 250 milligrams per liter; and *C*—after 47 days of withdrawal, when the computed chloride concentration of recovered water was about 750 milligrams per liter.

Methodology of Analysis

An analysis of multiple-well configurations required an areal model. The Cartesian coordinates version of the INTERA model was selected to represent a hypothetical single-layer aquifer having characteristics similar to those of the most permeable layer at the Hialeah site. Uniform 100×100 ft grid blocks comprised the interior of the 35×35 grid, and well configurations were centered in the grid. The resident fluid density was 62.57 lb/ft^3. The dispersion model of $\alpha_l = 4$ ft, $\alpha_t = 0$ used in all tests represented a relatively low level of longitudinal dispersion and no lateral transverse dispersion.

For multiple-well systems as well as for single wells, recovery may vary with the injection volume. So that well configuration effects would be isolated from other effects, the total volume of injection was the same (19,792,050 ft^3) in all tests except one. Generally, total injection and withdrawal rates were divided equally among all wells operating at a particular time.

Comparisons in the tests were among configurations and among injection and withdrawal schedules (table 1). In addition, all cases were compared with a control simulation of radial inflow and outflow from a single well, in which computed recovery efficiency was 83.1 percent. Row and column oscillations occurred during the

Table 1. Recovery efficiency computed for a variety of well configurations and injection and withdrawal schedules
[Rates in cubic feet per day]

Number of wells	Configuration	Injection schedule	Withdrawal schedule	Recovery efficiency
1	Centered in grid	329,867.5 for days 1–60	200,000	83.1
2	500 feet apart on Y-axis	Simultaneous; both wells—197,920.5, days 1–50	Simultaneous; each well at 100,000	82.4
2	do.	1 well—65,973.5, days 1–50; both wells—164,933.75, days 50–100	do.	81.7
3	Lined up 500 feet apart on Y-axis	Center well—65,973.5, days 1–50; all wells—109,955.81, days 50–100	Simultaneous; each well at 66,666.67	82.3
3	Triangular pattern, wells 500 feet apart	Simultaneous; all wells—131,947, days 1–50	do.	79.6
4	Triangular pattern, 500 feet apart with well in center	Center well—65,973.5, days 1–50; all wells—82,466.87, days 50–100	Simultaneous; each well at 50,000	82.0
4	Square array, 500 feet on each side	Simultaneous; all wells—98,960.25, days 1–50	do.	80.0
5	Center well with four wells 500 feet from center on each axis	Simultaneous; all wells—69,973.5, days 1–60	Simultaneous; each well at 40,000	74.0
5	do.	Center well—65,973.5, days 1–50; all wells—65,973.5, days 50–100	do.	82.5
5	do.	do.	Center well only at 200,000	77.3
5	do.	Smaller volume; center well—65,973.5, days 1–50; all wells—65,973.5, days 50–60	Simultaneous; each well at 40,000	58.2
7	Hexagonal pattern with center well; others 500 feet from center	Center well—65,973.5, days 1–50; all wells—47,123.93, days 50–100	Simultaneous; each well at 28,571.43	81.4
7	do.	do.	Simultaneous; each well at 40,000	81.5
9	Octagonal pattern with center well; others 500 feet from center	Center well—65,973.5, days 1–50; all wells—36,651.94, days 50–100	Simultaneous; each well at 22,222.22	81.4

computations, but results still showed the distribution of potable water with adequate clarity.

Two basic types of configurations, those with and without center wells, were simulated. Examples of configurations without center wells were the two-well system and the triangular and square arrangements. Adjacent wells were 500 ft apart. In the centered configurations, from two to eight wells surrounded a center well in a geometrically symmetric pattern. Each peripheral well was 500 ft from the center.

Exact symmetry could not be easily achieved in the triangular pattern or in the four-well, seven-well, and nine-well centered arrangements because grid nodes did not correspond exactly to the desired well locations. In the triangular and nine-well configurations, symmetry was achieved by representing some members of the configuration as pairs of wells at adjacent nodes, each with half the rate of that member of the configuration. In the four-well and seven-well configurations, wells correspond to grid nodes reasonably close to the desired locations, but exact symmetry was not achieved. This explains the bulge of potable water along the Y-axis which occurred during simulated injection in the seven-well configuration.

Two types of injection schedules were simulated, simultaneous and sequential. The simultaneous schedule consisted of common rates of injection at all wells of the configuration for the entire period of injection. This was simulated in the two-well, triangular, and square configurations, and also in the five-well centered configuration. The sequential injection schedule consisted of injection at a center well until the midpoint of the transition zone reached peripheral wells, 500 ft away. This was followed by injection at a common rate at all members of the configuration, including the center well, until the total volume common to all simulations had been injected. This schedule was simulated in the two-well configuration, with one well considered to be the "center" well, and in all of the configurations having a center well.

In most simulations, withdrawal was from all members of the configuration until various wells began to withdraw saline water. Following simultaneous injection schedules in the two-well, triangular, and square arrays, intrusion of saline water began at virtually the same time at all wells. This withdrawal schedule was approximately the inverse of the simultaneous injection schedule in that the pattern of inflow during withdrawal was the reverse of the pattern of outflow during injection. In the three- to nine-well centered configurations, peripheral wells became saline at virtually the same time but earlier than the center well, where withdrawal ceased at a later time. When this withdrawal schedule followed a sequential injection schedule in the centered configurations and in the two-well configuration, it approximated the inverse of the injection schedule. This was not true, however, for withdrawal following simultaneous injection in the five-well centered configuration.

Following one simulation of sequential injection into a five-well centered configuration, an alternative withdrawal schedule was simulated. Withdrawal was solely from the center well until it was invaded by saline water. In this case, the withdrawal schedule did not resemble the inverse of the injection schedule.

In one simulation of five-well sequential injection followed by multiple-well withdrawal, the total volume injected was only about one-third that of the other simulations. Two simulations of sequential injection and multiple-well withdrawal in the seven-well centered configuration used different withdrawal rates.

Results of Analysis

Recovery efficiencies for the various configurations and schedules of injection and withdrawal (table 1) show that the greatest degree of variation occurred when a smaller volume was injected in the five-well configuration. This is consistent with results of the single-well radial analysis of the relation between recovery efficiency and volume injected. However, when withdrawal rates were varied in the seven-well configuration, recovery efficiencies were virtually the same, supporting results of the single-well rate analysis.

Lines of equal pressure that correspond to injection or withdrawal at the various configurations of wells are shown in figures 15–18. Actual pressure levels are not shown, so as to generalize these depictions for injection or withdrawal at arbitrary rates. Figures 15–20 show the distribution of potable water for various configurations and schedules at the end of injection and at successive stages of withdrawal.

Sequential and simultaneous injection schedules in the two-well system (fig. 15) led to virtually the same recovery efficiency not much less than that of the single-well injection, though the distributions of potable water were different. When withdrawal followed a simultaneous injection schedule, saline water separated the two wells before withdrawn water became saline. In contrast, when withdrawal followed sequential injection, saline water reached the "peripheral" well, leaving it on the edge of a roughly circular body of freshwater surrounding the "center" well.

Simultaneous injection into the triangular and square configurations (figs. 16*A–C*, 17*A–C*) left stagnant saline water remaining within the configuration even after a large volume of freshwater had been injected (figs. 16*B*, 17*B*). This occurred because of flow troughs in the center of the two configurations and between adjacent wells in the square configuration. It is possible that this stagnant water might have been removed by processes of dispersion and entrainment, had simulated injection continued. Recovery efficiencies were slightly less than that of the single-well cycle (table 1). Slight amounts of potable water remained in storage, unrecoverable as such by the wells of the configuration, when withdrawn water became saline.

Generalized lines of equal pressure (figs. 16*D*, 17*D*, 18*A*) show somewhat more intense pressure gradients about the center well of the three-, four-, and five-well centered configurations than about the peripheral wells. The distribution of potable water at the end of sequential injection (figs. 16*E*, 17*E*, 19*A*, 20*A*, and 20*D*) becomes more nearly circular as the number of peripheral wells increases. Recovery efficiencies were only slightly less than for the single-well cycle (table 1) and were slightly greater than for the triangular and square configurations having no center well.

A comparison of figures 18*B* and 19*B* shows the different distributions of potable water at the end of simultaneous and sequential injection schedules in the five-well centered configuration, with the latter being more nearly circular. When multiple-well withdrawal followed simultaneous injection, the diminishing freshwater separated into five separate bodies surrounding each well (fig. 18*E*). When withdrawal ceased because of increasing

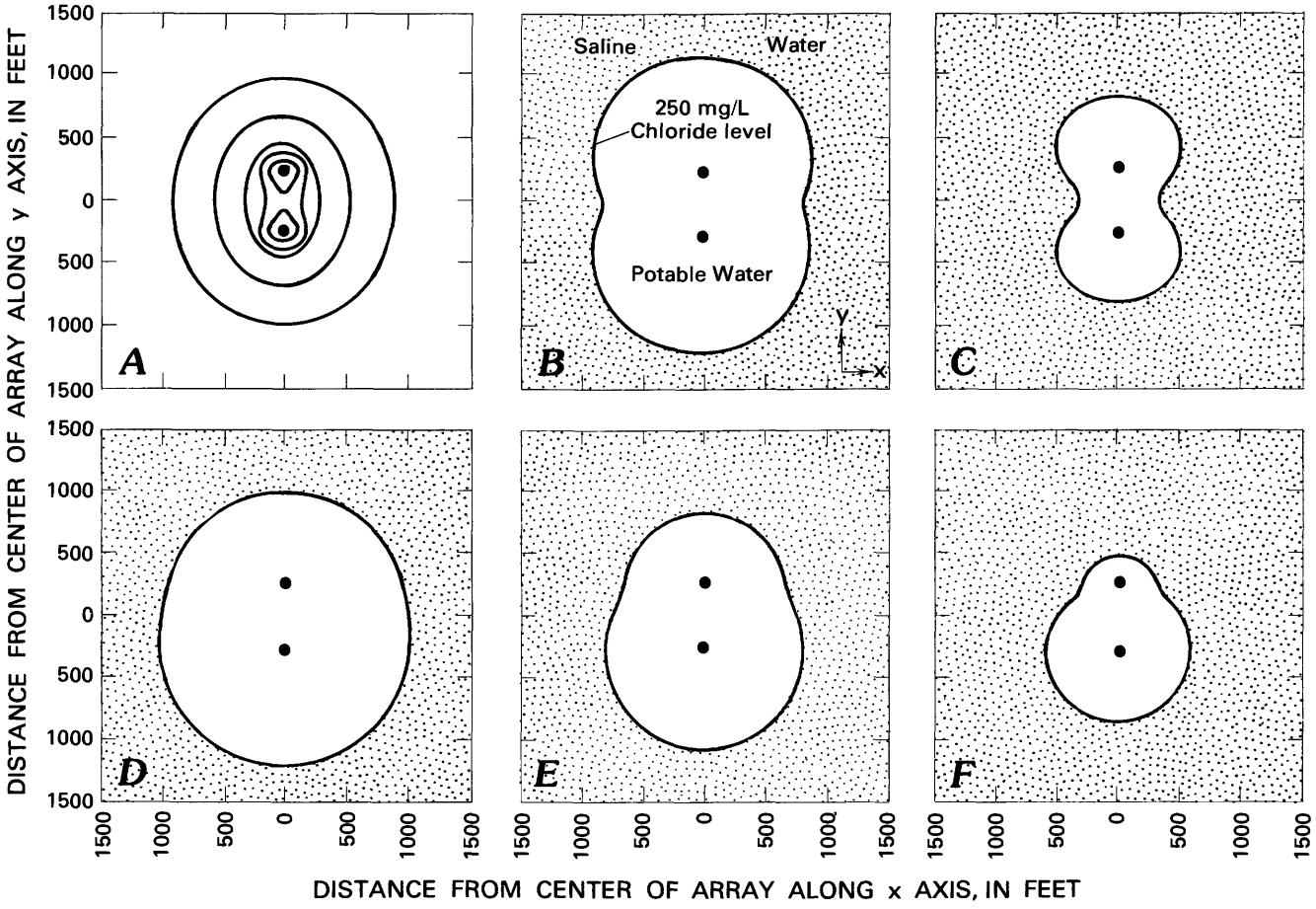

Figure 15. Pressure levels and the distribution of potable water during injection and withdrawal at two wells. Positions of injection/recovery wells in configuration are indicated by heavy dots. Shown are: *A*—generalized lines of equal pressure from injection or withdrawal at same rate at both wells, and potable water distribution: *B*—at end of simultaneous injection schedule; *C*—after 54 days of withdrawal at same rate from both wells following simultaneous injection schedule; *D*—at end of sequential injection schedule; *E*—after 34 days of withdrawal at same rate from both wells following sequential injection schedule; and *F*—after 58 days of withdrawal following sequential injection schedule.

salinity, pockets of potable water remained near the peripheral wells on the sides facing outward from the configuration (fig. 18*F*). Recovery efficiency was appreciably less than for the single-well cycle. When multiple-well withdrawal followed sequential injection, the diminishing freshwater mass remained undivided when the peripheral wells became saline (fig. 19*C*). Recovery efficiency was virtually as high as that of the single-well cycle. However, when withdrawal from only the center well followed sequential injection (figs. 19*D*, *E*), pockets of potable water remained near the peripheral wells on the sides facing into the configuration after the wells had become saline (fig. 19*F*). Recovery efficiency was appreciably less than that resulting from the multiple-well withdrawal following sequential injection.

It is of interest that when the withdrawal schedule did not approximately resemble the inverse of the injection schedule, recovery efficiency was appreciably less than that of the single-well cycle. This result correlates with the other circumstances (buoyancy stratification, drift caused by background hydraulic gradients, directionally biased plugging during injection) where the pattern of flow of freshwater back toward the well was dissimilar to its outward flow during injection. In each case, this was shown to reduce recovery efficiency. However, when injection and withdrawal schedules led to similar flow patterns, recovery efficiencies compared well with the single-well schedule, suggesting that these schedules in a centered configuration would be a satisfactory substitute if engineering considerations rendered a single-well injection facility infeasible.

SUMMARY AND DISCUSSION OF RESULTS

The INTERA three-dimensional, finite difference solute- and thermal-transport model was used to analyze

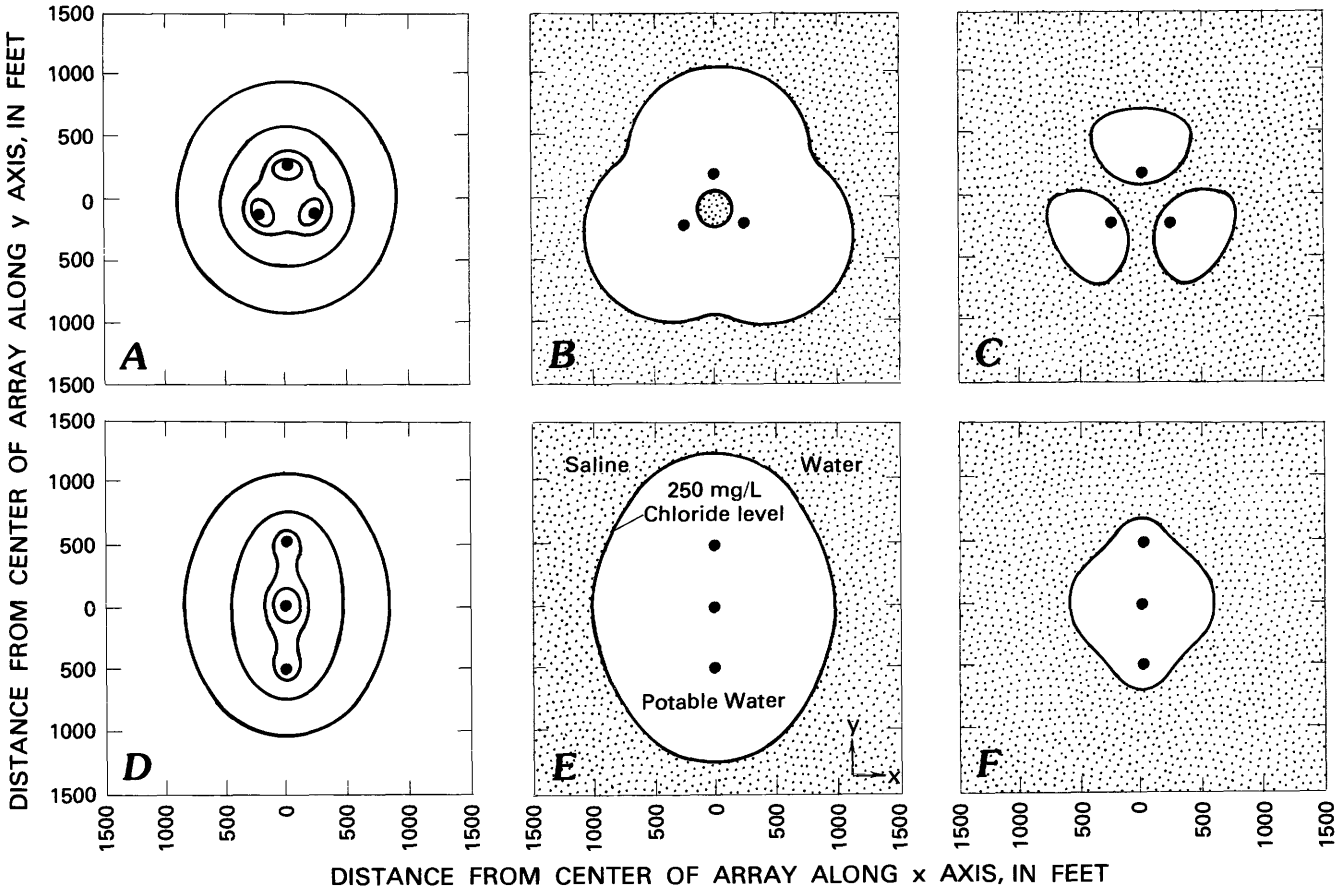

Figure 16. Pressure levels and the distribution of potable water during injection and withdrawal at two configurations of three wells. Positions of injection/recovery wells in configuration are indicated by heavy dots. Shown are: *A*—generalized lines of equal pressure from injection or withdrawal at same rate at three wells in triangular configuration; and potable water distribution: *B*—at end of simultaneous injection schedule, and *C*—after 54 days of withdrawal at same rate from all three wells following simultaneous injection schedule. Also shown are: *D*—generalized lines of equal pressure from injection or withdrawal at same rate at three wells in linear configuration; and potable water distribution: *E*—at end of sequential injection schedule, and *F*—after 58 days of withdrawal at same rate from all three wells following sequential injection schedule.

the relation of recovery efficiency to various hydrogeologic conditions that could exist in saline aquifers considered for storage of freshwater and to various design and operational aspects. The analyses consisted of a concept-testing approach, as opposed to the more familiar site-specific calibration, verification, and prediction objective of digital modeling. Cyclic injection in a hypothetical aquifer was simulated, incorporating computations for recovery efficiency. Sensitivity analyses were performed to determine how recovery efficiency varies when hydrogeologic or management parameters are varied. If the prototype aquifer of the control is considered representative of injection zones in an area such as south Florida, results show the relation to diverse conditions that might occur in that area. In this study, the Hialeah site was used as a prototype for the hypothetical aquifer. Since data from the tests did not determine the degree of dispersive mixing, various dispersion models were used in most analyses.

The INTERA model incorporated the assumption that the aquifer could be represented as uniform. The effect of small-scale flow heterogeneities in creating a transition zone at the interface between two fluids is represented by hydrodynamic dispersion terms. However, in aquifers with large-scale flow heterogeneities (large solution channels or conduits) which cannot be considered a continuum on the scale of the model, some of the model analyses may not apply, as processes affecting recovery efficiency might be considerably different from model assumptions.

Relation of Recovery Efficiency to Hydrogeologic Characteristics

The permeability of the aquifer is one factor that determines whether or not an appreciable degree of buoyancy stratification, a process that reduces recovery efficiency, can occur. Generally, low permeability reduces

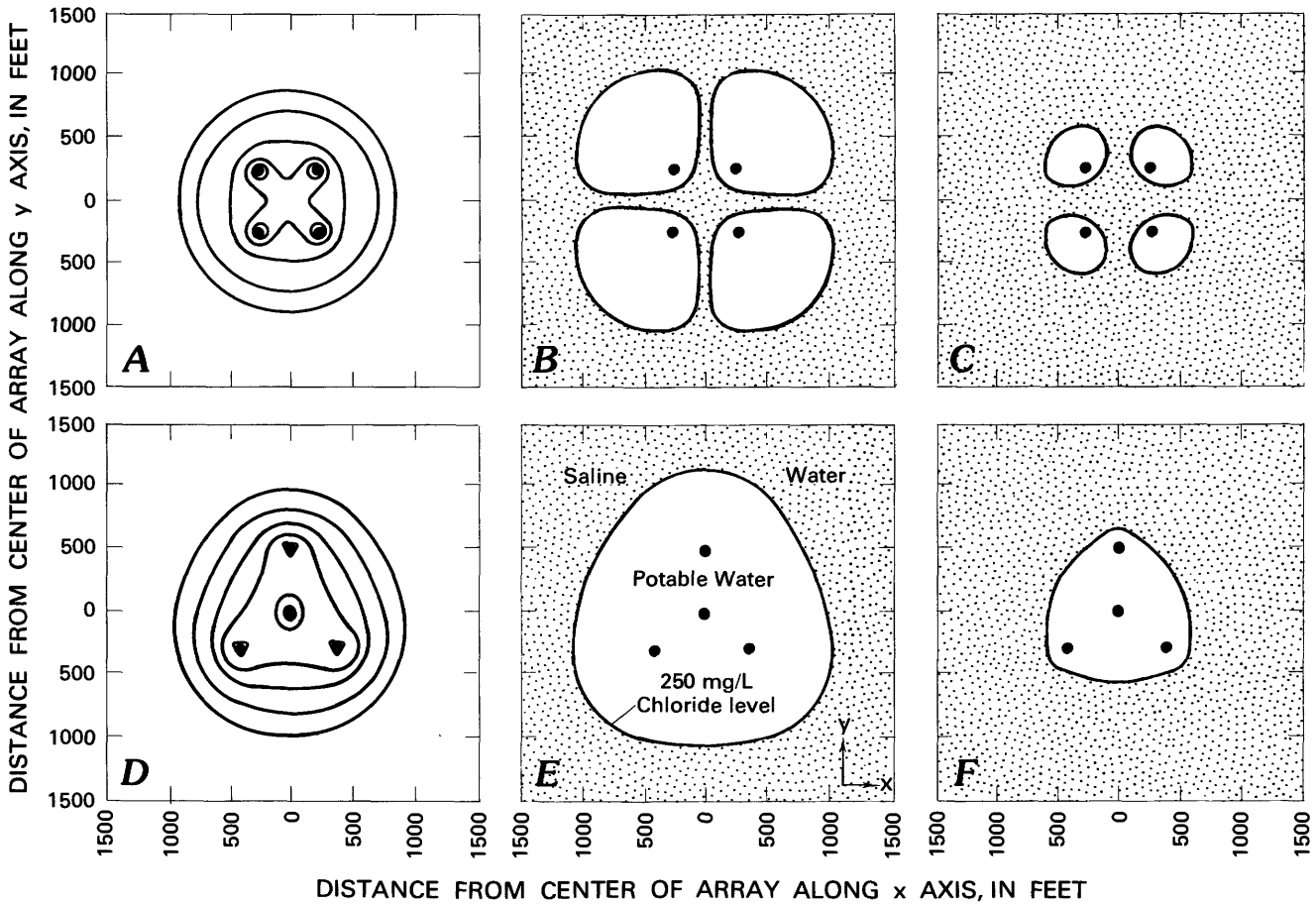

Figure 17. Pressure levels and the distribution of potable water during injection and withdrawal at two configurations of four wells. Positions of injection/recovery wells in configuration are indicated by heavy dots. Shown are: *A*—generalized lines of equal pressure from injection or withdrawal at same rate at four wells in a square configuration; and potable water distribution: *B*—at end of simultaneous injection schedule, and *C*—after 62 days of withdrawal at same rate from all four wells following simultaneous injection schedule. Also shown are: *D*—generalized lines of equal pressure from injection or withdrawal at four wells in a centered configuration; and potable water distribution: *E*—at end of sequential injection schedule, and *F*—after 58 days of withdrawal at same rate from all four wells following sequential injection schedule.

stratification and optimizes recovery efficiency. The permeability of the aquifer and the slightly brackish quality of the resident fluid of the injection zone at Hialeah were such that buoyancy stratification did not occur in simulations of injection, storage, or recovery. When the simulated permeability was increased by a factor of two or three, stratification was still negligible. However, if permeability had been 10 times greater, recovery efficiency would have been reduced 13.5 percent by buoyancy stratification. If the resident fluid had been more saline, appreciable buoyancy stratification would have been simulated in lower permeability ranges. In fact, when permeability values of the Hialeah site were used and the resident fluid was assumed to be as dense as seawater, buoyancy stratification caused the computed recovery efficiency to be about one-third less than if the permeability had been one-tenth as large.

Hydrodynamic dispersion is a major factor limiting recovery efficiency. Actual dispersion levels in the saline artesian zones of south Florida are not well known. Recovery efficiency decreases appreciably as the level of dispersive mixing increases, as a greater volume of freshwater combines with saline water in a nonpotable mixture.

As the salinity of the resident fluid increases, a smaller volume of water within the transition zone caused by hydrodynamic dispersion is potable. Thus, recovery efficiency was shown in model analyses to be less in highly saline aquifers than in moderately saline aquifers. Higher salinity also makes buoyancy stratification more

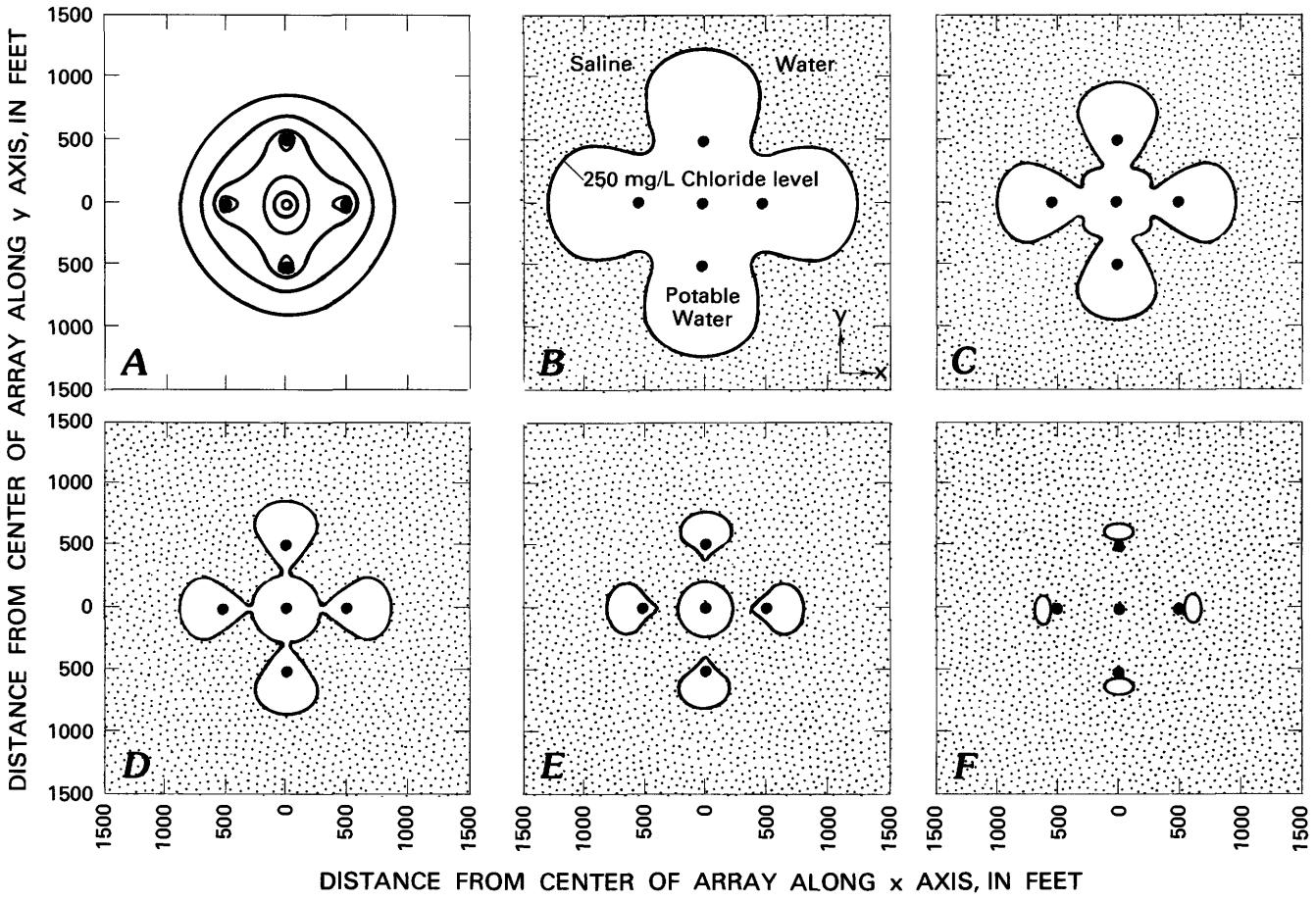

Figure 18. Pressure levels and the distribution of potable water resulting from simultaneous injection at a centered configuration of five wells. Positions of injection/recovery wells in configuration are indicated by heavy dots. Shown are: *A*—generalized lines of equal pressure from injection or withdrawal at same rate at the five wells; and the distribution of potable water: *B*—at end of simultaneous injection schedule, *C–E*—after 42, 54, and 62 days of withdrawal at same rate from all five wells following simultaneous injection schedule, and *F*—after withdrawal ended because recovered water exceeded 250 milligrams per liter of chloride at all wells.

likely to occur for any given degree of permeability, decreasing recovery efficiency. Thus, aquifers containing water just saline enough to be unsuitable for consumption are optimum for freshwater injection and recovery, and highly saline aquifers are least promising.

In model analyses in which interlayer dispersion (dispersion into adjacent, less permeable layers still containing native saline water at radii reached by freshwater in the more permeable layer) was represented as being negligible, recovery efficiency was somewhat greater in thin layers than in thick layers. Model computations of recovery efficiency where layer thickness was quadrupled showed a 10.6 percent decrease with no interlayer dispersion and a 72.2 percent improvement with some interlayer dispersion. The variations were the result of differences in the degree of dispersion occurring for different layer thicknesses and porosities. Storage capacity, particularly the zonal thickness factor, may determine, for a given volume of injected freshwater, whether regional flow can significantly move the freshwater during a period of storage.

Background hydraulic gradients can reduce recovery efficiency by conveying the stored freshwater downgradient. In most saline aquifers, the only background gradient is the natural regional one. In the injection zone at the Hialeah site, the estimated regional hydraulic gradient of 10 to 20 ft in 45 miles is too small to appreciably displace a large amount of injected freshwater during 6 months of storage. However, simulations involving a 5-year storage period showed recovery efficiency at the site to be greatly reduced. Substantial potable water would remain in the aquifer unrecoverable by the injection well, though a downgradient well could recover additional potable water. Generally, the effect of storage periods of various lengths on recovery efficiency depends on site-specific hydrogeologic factors such as permeability and layer thickness and on the volume of freshwater injected.

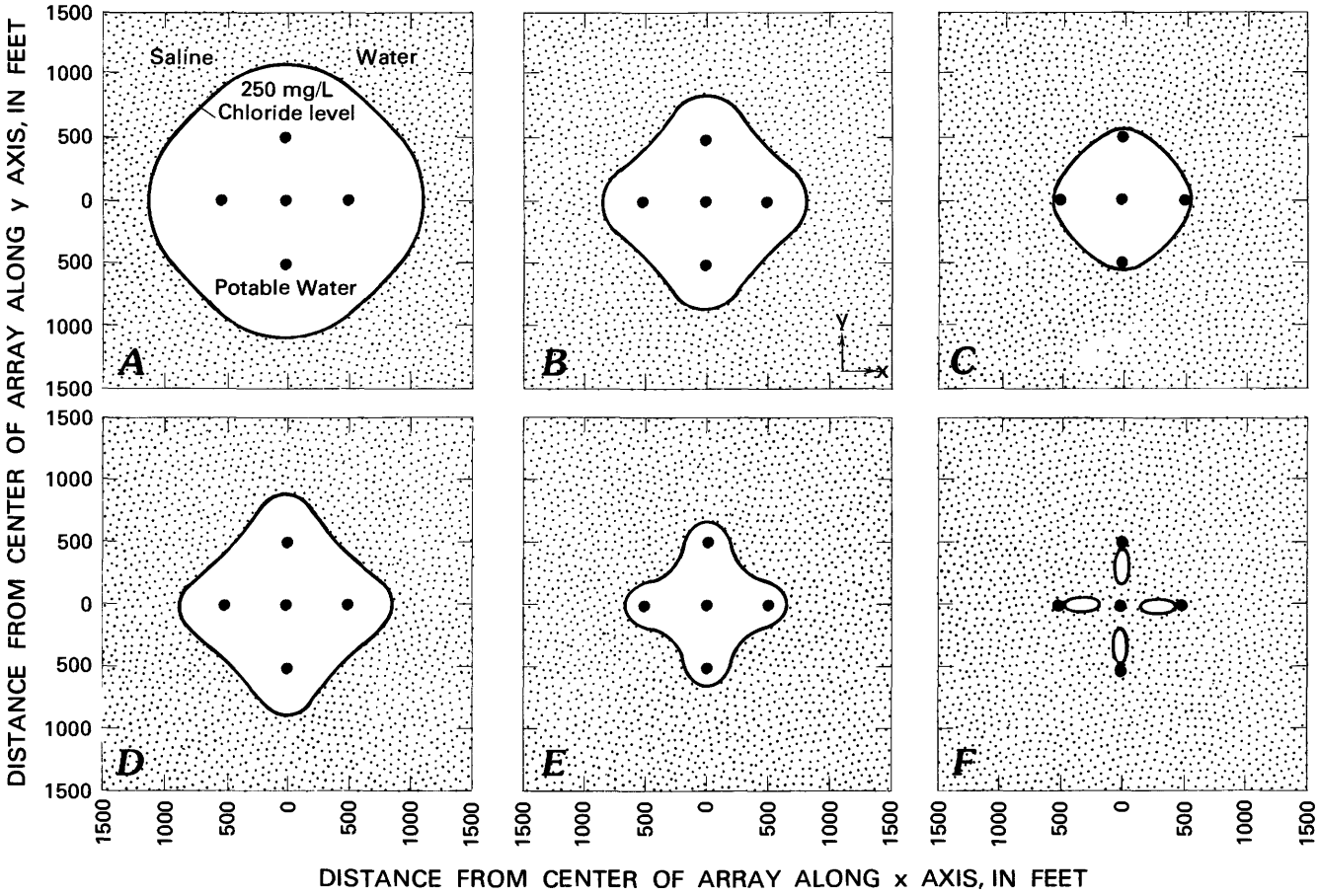

Figure 19. The distribution of potable water resulting from a sequential injection schedule and alternative withdrawal schedules at a centered configuration of five wells. Position of injection/recovery wells in configuraton are indicated by heavy dots. Shown are the distribution of potable water: *A*—at end of sequential injection schedule; *B*, *C*—after 42 and 62 days of withdrawal at same rate from all five wells following sequential injection schedule; *D*, *E*—after 42 and 62 days of withdrawal from center well alone at a rate equal to the combined rates of *B* and C; and *F*—after withdrawal from center well alone ended because recovered water exceeded a chloride concentration of 250 milligrams per liter.

Relation of Recovery Efficiency to Design and Management Parameters

The rate at which a given volume of freshwater is injected or recovered apparently does not affect recovery efficiency. When the injection rate was increased by an order of magnitude and the time of injection decreased by an order of magnitude, the simulation of the structure of the transition zone and computed values of recovery efficiency remained the same. When an injection and recovery well was represented as open only to part of a permeable zone, recovery efficiency was virtually the same as when the well was open to the entire zone, although the pattern of flow to and from the well was altered. Simulations indicated that the length of storage has no effect on the recoverability of the injected freshwater, provided that (1) regional ground-water flow does not appreciably displace the stored freshwater in the interim, and (2) appreciable buoyancy stratification cannot occur under prevailing hydrogeologic conditions. Generally, recovery efficiency improves with increased volume. Exceptions were related to the simulation of small degrees of interlayer dispersion.

Recovery efficiency improves with repeated cycles, if each withdrawal phase is stopped when withdrawn water reaches a limiting salinity value (250 mg/L of chloride). Recovery efficiency improved rapidly in initial cycles and then more slowly until it was nearly constant after the 12 cycles that were simulated with the model. The 12-cycle efficiency value depended on the degree of dispersion in the direction of flow, higher efficiencies being reached for lower degrees of dispersion. When a low level of interlayer dispersion was represented, recovery efficiency was low initially but rapidly improved with repeated cycles until it was nearly the same as when no interlayer dispersion was simulated.

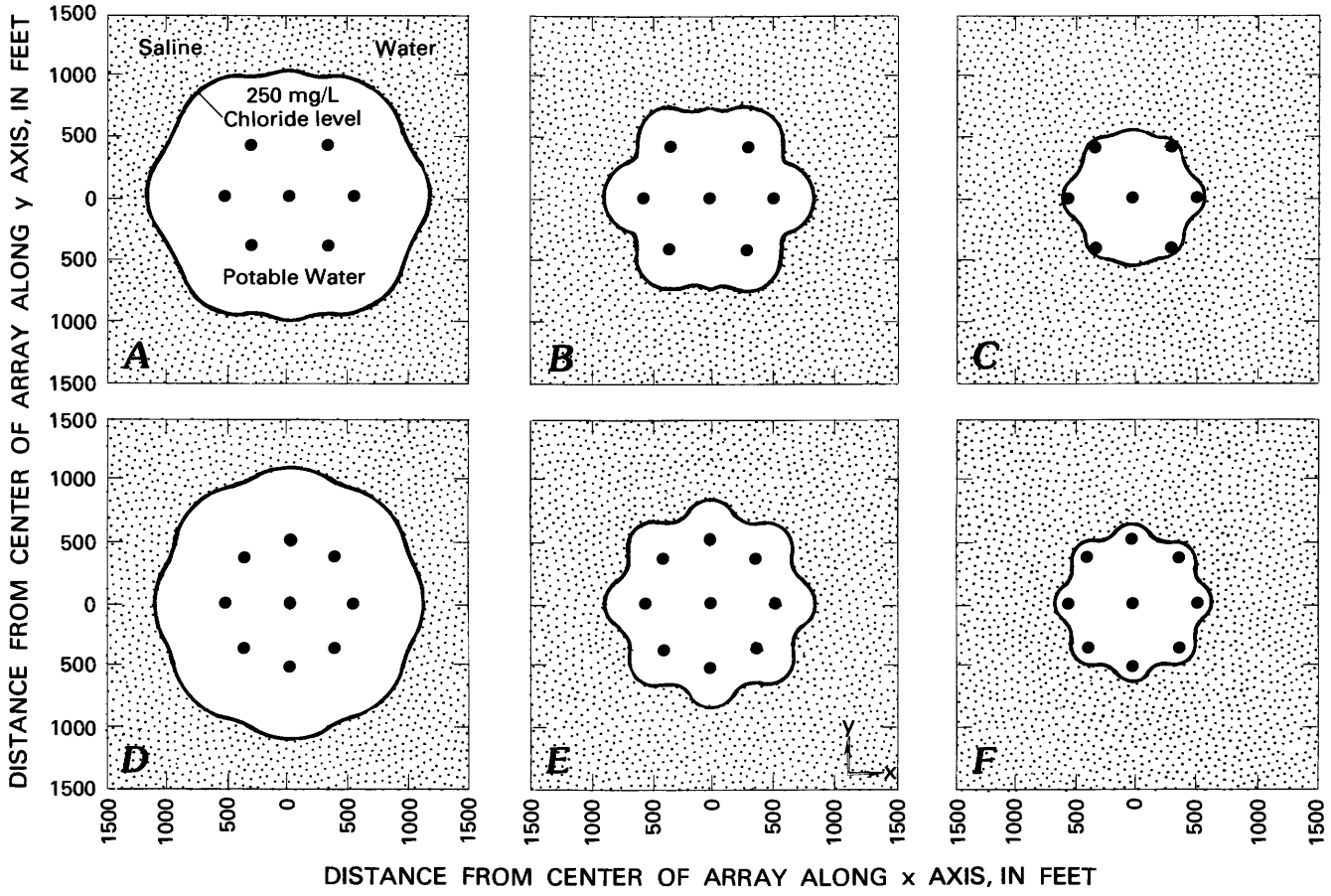

Figure 20. The distribution of potable water resulting from injection and withdrawal at centered configurations of seven and nine wells. Positions of injection/recovery wells in configuration are indicated by heavy dots. Shown are the distribution of potable water: *A*—at end of sequential injection schedule at seven wells in a centered configuration; *B*, *C*—after 42 and 62 days of withdrawal at the same rate from all seven wells following the sequential injection schedule; *D*—at end of sequential injection schedule at nine wells in a centered configuration; and *E*, *F*—after 42 and 58 days of withdrawal at the same rate at all nine wells following the sequential injection schedule.

Recovery efficiency can be reduced if the spatial distribution of permeability changes because of well-bore plugging during injection. If such a process occurs, potable water would be left unrecoverable as such in the aquifer after withdrawn water became saline. Model tests were designed with permeability along one axis within the plane of flow reduced during the injection phase to 10 percent of its nominal value. Recovery efficiency was reduced to about one-third of the value it had in control simulations in which this change of permeability was not simulated.

Model tests of various multiple-well configurations and injection and withdrawal schedules permitted a selection of those producing the best recovery efficiencies. Withdrawal schedules should resemble the inverse of the injection schedules. Greatest efficiencies were achieved in configurations consisting of a central well surrounded by perimeter wells. Injection was into the central well until freshwater reached the perimeter wells, at which time injection at equal rates continued at all wells (sequential injection schedule). Withdrawal was at equal rates at all wells, the perimeter wells were shut down first when withdrawn water became saline, and the central well was shut down later when it also became saline. The number of perimeter wells was varied from one to eight with little effect on recovery efficiency, which for these configurations and schedules was nearly the same as if injection and withdrawal had been from a single well.

Simultaneous, equal-rate injection and withdrawal in configurations having no central well led to only slightly lower recovery efficiency than sequential injection in centered configurations, but this schedule in a configuration having a central well led to an appreciable decrease in recovery efficiency from that of the sequential injection schedule. When withdrawal from only the central well followed a sequential injection schedule, recovery efficiency was appreciably reduced.

Significance of Study

Generally, it was shown that a loss of recovery efficiency was caused by (1) processes causing mixing of injected freshwater with native saline water (hydrodynamic dispersion), (2) processes causing the more or less irreversible displacement of the injected freshwater with respect to the well (buoyancy stratification, background hydraulic gradients, interlayer dispersion), or (3) processes causing injection and withdrawal flow patterns to be dissimilar (directionally biased well-bore plugging, dissimilar injection and withdrawal schedules in multiple-well systems). A significant result was the theoretical demonstration that recovery efficiency should improve considerably with successive cycles, provided that each recovery phase ends when the chloride concentration of withdrawn water exceeds established criteria for potability (usually 250 mg/L).

A wide range of hydrologic conditions have been posed for model analysis, and results have illustrated many relations showing the effect of such conditions on the recoverability of injected freshwater. To have obtained these results with operational testing would have been orders of magnitude more costly. The tradeoff is that the validity of results obtained from computer modeling are somewhat less certain. In particular, results must be qualified with observations that (1) the complex set of processes lumped as hydrodynamic dispersion are represented with a somewhat simplified mathematical approximation, and (2) other flow processes in limestone injection zones are as yet incompletely understood. These qualifications mean that some degree of uncertainty remains concerning the appropriateness of the representation of flow and transport processes in limestone in currently available digital models. Despite such reservations, the study is considered a practical example of the use of transport models in ground-water investigations, and should aid understanding of how to realistically and effectively use solute-transport models.

REFERENCES CITED

Bear, J., 1972, Dynamics of fluids in porous media: New York, American Elsevier Publishing Co., 764 p.

Ehrlich, G. G., Godsy, E. M., Pascale, C. A., and Vecchioli, John, 1979, Chemical changes in an industrial waste liquid during post-injection movement in a limestone aquifer, Pensacola, Florida: Ground water, v. 17, no. 6, p. 562–573.

Grove, D. B., and Konikow, L. F., 1976, Modeling cyclic storage of water in aquifers: Abstract presented to the American Geophysical Union, San Francisco, Calif., December, 1976.

Hoopes, J. A., and Harleman, D. R. F., 1967, Dispersion in radial flow from a recharge well: Journal of Geophysical Research, v. 72, no. 14, p. 3595–3607.

INTERA Environmental Consultants, Inc., 1979, Revision of the documentation for a model for calculating effects of liquid waste disposal in deep saline aquifers: U.S. Geological Survey Water-Resources Investigations 79–96, 73 p.

INTERCOMP Resource Development and Engineering, Inc., 1976, A model for calculating effects of liquid waste disposal in deep saline aquifers, Part 1—Development, Part 2—Documentation: U.S. Geological Survey Water-Resources Investigations 76–61, 253 p.

Khanal, N. N., 1980, Advanced water supply alternatives for the Upper East Coast Planning Area, Part I—Feasibility of cyclic storage of freshwater in a brackish aquifer, Part II—Desalinization alternative: South Florida Water Management District Technical Publication 80–6, 75 p.

Kimbler, O. K., Kazmann, R. G., and Whitehead, W. R., 1975, Cyclic storage of freshwater in saline aquifers: Louisiana Water Resources Research Institute Bulletin 10, 78 p.

Klein, Howard, Armbruster, J. T., McPherson, B. F., and Freiberger, H. J., 1974, Water and the south Florida environment: U.S. Geological Survey Water-Resources Investigations 75–24, 165 p.

Konikow, L. F., and Grove, D. B., 1977, Derivation of equations describing solute transport in ground water: U.S. Geological Survey Water-Resources Investigations 77–19, 30 p.

Lantz, R. B., 1971, Quantitative evaluation of numerical diffusion (truncation error): Society of Petroleum Engineers Journal, September 1971, p. 315–320.

Lau, L. K., Kaufman, W. F., and Todd, D. K., 1959, Dispersion of a water tracer in radial laminar flow through homogeneous porous media: Progress report 5, Canal Seepage Research, Hydraulic and Sanitary Engineering Research Laboratories, University of California.

Leach, S. D., Klein, Howard, and Hampton, E. R., 1972, Hydrologic effects of water control and management of southeastern Florida: Florida Bureau of Geology Report of Investigations 60, 115 p.

Lohman, S. W., 1979, Ground-water hydraulics: U.S. Geological Survey Professional Paper 708, 70 p.

Merritt, M. L., 1982, Subsurface storage of freshwater, south Florida: ASCE National Specialty Conference on Environmentally Sound Water and Soil Management, Orlando, Fla., July 1982, Proceedings, p. 242–250.

Merritt, M. L., Meyer, F. W., Sonntag, W. H., and Fitzpatrick, D. J., 1983, Subsurface storage of freshwater in south Florida: A prospectus: U.S. Geological Survey Water Resources Investigations Report 83–4214, 69 p.

Pinder, G. F., and Gray, W. G., 1977, Finite element simulation in surface and subsurface hydrology: Academic Press, New York, 295 p.

Price, H. S., and Coats, K. H., 1973, Direct methods in reservoir simulation: SPE 4278 presented at the Third SPE Symposium on numerical simulation of reservoir performance of SPE of AIME, Houston, Tex., January 11–12, 1973.

Price, H. S., Varga, R. S., and Warren, J. E., 1966, Application of oscillation matrices to diffusion-convection equations: Journal of Mathematics and Physics, v. 45, p. 301–311.

Reeder, H. O., Wood, W. W., Ehrlich, G. G., and Ren Jen Sun, 1976, Artificial recharge through a well in fissured carbonate rock, West St. Paul, Minnesota, with a chapter on Hydrodynamic dispersion and movement of injected water by Ren Jen Sun: U.S. Geological Survey Water-Supply Paper 2004, p. 52–75.

Scheidegger, A. E., 1961, General theory of dispersion in porous media: Journal of Geophysical Research, v. 66, no. 10, p. 3273–3278.

Sonntag, W. H., 1984, Subsurface storage of freshwater in south Florida: Evaluation of surface-water discharge data at selected sites: U.S. Geological Survey Water-Resources Investigations Report 84–4008, 75 p.

U.S. Environmental Protection Agency, 1977, Quality criteria for water, 1976: 256 p.

Wheatcraft, S. W., and Peterson, F. L., 1979, Numerical modelling of liquid waste injection into a two-phase fluid system: University of Hawaii at Manoa, Water Resources Research Center Technical Report 125, 103 p.

METRIC CONVERSION FACTORS

For readers who prefer to use metric units, conversion factors for terms used in this report are listed below:

Multiply	By	To obtain
in (inch)	25.4	mm (millimeter)
ft (foot)	0.3048	m (meter)
mi (mile)	1.609	km (kilometer)
ft^3 (cubic foot)	0.0283	m^3 (cubic meter)
ft/d (foot per day)	0.3048	m/d (meter per day)
ft^2/d (square foot per day)	0.0929	m^2/d (square meter per day)
ft^3/d (cubic foot per day)	0.0283	m^3/d (cubic meter per day)
ft/y (foot per year)	0.3048	m/y (meter per year)
gal/min (gallon per minute)	0.0631	L/s (liter per second)
gal/d (gallon per day)	0.0038	m^3/d (cubic meter per day)
lb/in^2 (pound per cubic foot)	6.895	kPa (kilopascal)
lb/ft^3 (pound per square inch)	16.02	kg/m^3 (kilogram per cubic meter)

National Geodetic Vertical Datum of 1929 (NGVD of 1929): A geodetic datum derived from a general adjustment of the first-order level nets of both the United States and Canada, called NGVD of 1929, is referred to as sea level in this report.